TU DELFT

Distributed temperature sensing for landfill monitoring and research

by

Rahul Sai Nambiar

Student Number-4511301

A thesis submitted in partial fulfilment of the
degree of Master of Science

Geotechnical Engineering
Faculty of Civil Engineering and Geosciences

Thesis Committee

Prof.Timo.J.Heimovaara Prof.Susan Steele-Dunne Prof.Wout Broere

December 2017

Acknowledgements

Firstly, I would like to express my gratitude to my thesis supervisor, Prof.Timo.J.Heimovaara, who provided me with the opportunity to conduct this 'one of a kind research' for the environmental geo-technics department at TU Delft. Besides Timo, I would like to thank the rest of my thesis committee: Prof.Wout Broere and Prof.Susan Steele-Dunne, for their feedback and comments. They consistently allowed this paper to be my own work, while steering me in the right direction whenever they believed I needed it and thereby helping me in overcoming the numerous obstacles I had to face throughout my research.

My sincerest thanks also go to Dr.Andre Van Turnhout, my daily supervisor. Without his support, it would have been not possible to conduct this research. Andre was just a text message away whenever I ran into a trouble spot or had a question about my research or writing. His continuous support, patience, motivation, and immense knowledge in various fields helped me formulate useful research strategies. His guidance helped me at all times during this research and while writing the thesis. I would also like to thank the experts who were involved in setting up this field for this research project, namely Han and Jens. Without their passionate participation and input, this research could not have been successful.

Finally, I must express my very profound gratitude to my family and to my friends for providing me with unfailing support and continuous encouragement throughout my years of study and through the process of researching and writing this thesis. This accomplishment would not have been possible without them. Thank you.

Rahul Sai
Delft, December 2017

Abstract

Reduction of emission potential of landfills has long been an area of study in the field of environmental geotechnics. Emission potential can be partly, indirectly inferred from temperatures within a landfill which indicate the bio-activity within a landfill. Temperatures can also indicate the effectiveness of treatments applied on landfills to reduce the emission potential. Predicting the thermal behaviour of landfills by modelling contains a degree of uncertainty because of the heterogeneous nature of waste bodies. Heat flow models have been developed to try and simulate the processes occurring within the landfill. In the past, models were validated with the aid of discrete temperature sensors at predetermined locations. The data sets obtained had to be interpolated to achieve a finer resolution of temperature profiles, and temperatures were highly variable because of the heterogeneity. In this study we aim to decrease the uncertainty in temperature measurements at field scale by evaluating a Distributed Temperature Sensing (DTS) system. This method is said to provide a higher resolution of temperature directly. In order to determine the effectiveness of the system, three fields around the Netherlands have been installed with DTS. The system was calibrated using a series of different tests and settings. Baseline measurements are made at the pilot locations, and are presented in the context of a detailed analysis. Also, temperature profiles after aeration treatment applied at the pilot are shortly discussed. Finally, some recommendations are discussed on how to make maximum use of this new technology for future research projects.

Contents

List of Figures

List of Tables

List of Symbols

x	position (m)
a	length (m)
b	length (m)
c	length (m)
$z1$	position (m)
$z2$	position (m)
$sd1$	length (m)
$sd2$	length (m)
i	index value (-)
k	Thermal conductivity (W/mK)
α	Thermal Diffusivity (m^2/day)
ρ_{bw}	Wet Bulk Density (kg/m^3)
C_p	heat capacity (MJ/m^3K)
q	heat ($J\ /m^2s$)
H	heat (J)
T	temperature (deg C)
$A(i,t)$	temperature (deg C)
t	time (days)

Chapter 1

Introduction

Municipal Solid Waste (MSW) landfills emit pollutants via gas and leachate over extended periods which puts a significant burden on future generations. To protect human health and the environment from these emissions, long-term after-care of landfills is required. Most of the landfills have reached their full capacity and need methods to reduce their harmful environmental impact and thereby to shorten their after-care.

It can take hundreds of years before the emissions from a landfill reach acceptable levels because the degradation and transport processes responsible for the emissions are very slow. The goal of sustainable land-filling concerning the European regulatory framework is to meet the emission thresholds for a landfill for inert waste within about 30 years as well as not to exceed the threshold values for groundwater quality [1]. Having considered that biological decomposition in a landfill is a slow process the aim is to enhance this process by applying treatment methods.
Aeration is a treatment method that introduces several benefits for shortening after-care. The (partly) aerobic conditions significantly reduce methane emissions, decreasing the impact on global warming. Aerobic bio-degradation is, in general, faster than anaerobic degradation [2] and neutralizes pollutants which are not reactive under anaerobic conditions. Aeration also reaches more biodegradable carbon within the heterogeneous waste-body than other treatment methods such as leachate re-circulation [3]. A potential risk of applying aeration is that it could lead to elevated temperatures within the landfill. Aerobic digestion is an exothermic process which generates a lot of heat, which could lead to dangerous landfill fires. Therefore, it is essential to monitor temperatures within the waste-body during aeration carefully.
A major challenge in applying treatments on a full scale is to assess their effectiveness in reducing emission potential. After-care of a landfill can only be brought to an end when sufficient evidence is conclusive that future long-term emissions remain low. Prediction

of emission potential, is governed by a multitude of factors and is difficult to correctly predict due to the heterogeneous nature of the waste-body and the minimal availability of effective measurement techniques. Over the years, quite a lot of research has therefore been carried out to formulate models that allow predicting the emission potential of a landfill from the scarcity of available measurements. In these models, coupled together are the processes of water flow, mass exchange, and bio-degradation within a single framework [3]. Models often consist of differential equations, which formulate the exchange of materials, energy or other quantities between model compartments (the state variables) on the basis of mass conservation principle [4].

To further improve model calibration, enhanced full-scale measurement techniques are needed. . Temperature are (indirectly) related to multiple processes such as water flow (heat content of water) and biological activity (reaction enthalpy) [5]. A high-resolution measurement can therefore significantly reduce model uncertainty. Besides, it also enables careful monitoring of temperature increase during aeration.

Temperature measurements have been performed at a full scale on landfill and have contributed substantially to model development so far. Discrete measurement techniques limit the resolution, accuracy, and geometry that can be achieved on field. These limitations, however, can be overcome by applying the upcoming technology of Distributed Temperature Sensing (DTS). DTS has been used successfully in many fields, namely oil and gas industry, Power Systems, Structural health monitoring, aviation etc [6]. One of its first applications was at deep wells (over 1km) to acquire real-time monitoring of temperatures and possible leaks [7]. Since its first implementation more than a decade ago, the technology has seen improvements regarding spatial and temporal resolution. The technology provides a continuous sensing network with the aid of fibre optic cables. These cables can be configured to attain a sampling interval as high as 25cm whereas, point sensors can limit the speed, accuracy, and resolution of monitoring in many applications. Distributed sensing relies on analysis of light pulses reflected down optical fibres and offers a better and more efficient way to monitor changes in temperature.

The fiber optic monitoring system may be also a valuable tool for locating problematic points in liquid injection systems and evaluating the effect of leachate injection on moisture conditions [8], and can be extended to aeration systems to monitor their effects.

The objective of this research is to determine too what extent DTS can enhance temperature readings within a landfill. After the installation of a 3-dimensional DTS grid at three pilot locations on landfills, we evaluate the accuracy, reproducibility, and resolution of the temperature readings. Comparisons of obtained readings are made with analytical formulations to check the applicability of the system for future monitoring and research.

Chapter 2

Background theory

2.1 Heat and landfills

Leachate, gas, and heat are the three most common byproducts of organic waste decomposition in landfills [9]. The decomposition of organic wastes occurs in three phases: anaerobic phase, a transient phase, and an aerobic phase. Heat generation takes place in all these phases and research suggests that most of the production takes place during the transient and anaerobic stage [10]. The heat evolved during these stages are also dependent on factors such as the waste placement rate, seasonal temperature variation and precipitation rate. Both the waste placement rate and precipitation have a positive co-relation to heat content of the soil and the annual temperature variations are mostly captured in the top layers of the landfill [9]. Landfills will show changes in temperature during the process of aeration [11]. It is in the best interest of the landfill operators and the researchers to monitor the changes in temperature during the aeration phase. Landfills can heat upto to 50-60 degrees during aeration and such activity can lead to landfill fires. This imposes a threat both to the environment and personnel on field and hence require an efficient temperature measurement system.

Change in heat content or temperature within the landfill can be attributed to a combination of certain processes. Heat generation can be estimated using the field temperature data and an analytic heat transfer formulation. The energy required to raise the temperature of waste depends on the heat capacity of the waste and the magnitude of temperature increase of the waste. Factors that influence heat content are the evaporation of water, the enthalpy released by the biochemical reactions, and the heat loss to the surrounding environment [9].

The impact of these different processes can all be combined into a generic heat equation:

$$\rho_{bw} C_p \frac{dT}{dt} + \bigtriangledown q_h + S = 0 \tag{2.1}$$

where ρ_{bw} is the wet bulk density of the porous system $[kg/m^3]$, C_p is the heat capacity of the bulk material $[Jkg^1K^1]$, T is the temperature of the material$[K]$, S can be considered the as a sink or source term and $\bigtriangledown q_h$ is the heat flux.

$$q_h = \bigtriangledown(-k \bigtriangledown T) \tag{2.2}$$

where k is the thermal conductivity $[W/(mK)]$ and $\bigtriangledown T$ is temperature gradient.

The source term here can be considered to be a function of biological activity, which results in decomposition and bio-chemical reactions that produce heat. The heat flux is strongly affected by convection due to the flow of water and diffusion due to temperature gradients. A value of zero was selected for the source term in the 1D heat transfer model that is used as a comparison.
Water has a crucial role to play in the distribution of heat. Considering heat flow mechanisms it is also possible for heat to flow by thermal convection due to infiltration of water. As cold water moves from the surface towards the ground it is possible for the water to absorb a certain amount of heat as it percolates through the depth of the landfill. Considering the heterogeneous nature of the soil it is also possible for the water to be retained within pockets inside the landfill. Convection is the movement of heat from one place to another through the movement of fluids. Water being the fluid under consideration here, can cause some thermal changes, one by flow of water and secondly,(as moisture) by enhancing biological activity. In an anaerobic environment, it can be hypothesized that the hotter regions in the deeper regions of the landfill are a result of water retention and subsequent increased biological activity.

As a consequence, the dynamics of water and thermal energy become closely coupled. This situation becomes even more complicated at a waste disposal site, with modified thermal properties and artificial heat sources as a result of material heterogeneity.

Along with the Richards equations a basic coupled model for heat and water flow can be formulated. Research suggests the cable temperatures could be used to estimate soil thermal properties from which soil moisture could be inferred [12].

The waste decomposition process is primarily a biological process which produces enthalpy. Enthalpy, in this case, is the heat released during biochemical reactions, which can be formulated into equations.

$$H_o^{reaction} = \sum \Delta H_o^f(products) - \sum \Delta H_o^f(reactants) \tag{2.3}$$

Where H_o^f is the standard symbol for enthalpy of formation.
This equation essentially states that the standard enthalpy change of formation is equal to the sum of the standard enthalpies of formation of the products minus the sum of the standard enthalpies of formation of the reactants. By doing so we can break down the biological reactions down to simple chemical reactions(hydrolysis, methanogenisis, oxidation).

Temperature can be related to the fraction of total biochemical energy used to heat the landfill. The resulting equation [13] for temperature change is presented below:

$$\Delta T = \frac{\Delta H}{C_p M(T)} \tag{2.4}$$

where H=energy production(heat generation)(MJ/m^3) from previous equation, ΔT=increment of temperature rise for waste (K); c=heat capacity of waste (MJ/m^3K); and M(T)=fraction of energy released that is used for heating a landfill [9].
The energy produced from biological activity can be estimated by considering few key equations that are dominant within a landfill namely hydrolysis, methanogenesis, bacterial decay and (de)nitrification [3]. Temperatures variations within the soil cover [14] has been thoroughly studied. Variations in temperature profile trends at different sites conclude that soil cover temperatures are a function of the air temperature and solar radiation.
Another important heat source noticeable within a landfill is the effect of radiation from the sun on the surface temperature and its subsequent diffusion into the soil. Research [9][10] suggest there is an effect of seasonal variations in temperature and the influence of the suns radiation, noticeable in the soil cover. The provided background theory can be used to quantify the heat within the landfill system.

A program in Matlab that solves the Heat Diffusion Equation 2.1 for a 1D soil profile using a finite difference approximation scheme was created. The 13m soil column was discretised into cells of 0.1m each. The top boundary condition of this scheme was taken as a simulation of the temperature change throughout a year:

$$T_0 = T_{avg} - T_{range}\cos(2\pi(\frac{t - t_{min}}{365}) \tag{2.5}$$

where T_{avg} is the average temperature taken as 10 deg C, T_{range} is the temperature amplitude assumed as 15 deg C and $t_{min} = 46$ is the number of days after the start of the year that the temperature reaches its minimal value. The bottom boundary conditions is a zero gradient condition (i.e. no diffusion flux). The above equations have been implemented using an implicit Euler approach, which we choose to solve using Matlab ODE solvers.

2.2 DTS

Distributed thermal sensing is a technology that enables continuous, real-time temperature measurements along the entire length of a fibre optic cable. Unlike traditional sensors, that rely on discrete sensors measuring at pre-determined points, distributed sensing does not rely upon manufactured sensors, but utilizes the optical fibre. The optical fibre is the sensing element without any additional devices in the optical path.

A DTS system obtains temperature readings along the length of its fiber optic cable. The cable can stretch as much as 10km and can provide a temperature reading of spatial resolution 25cm in a short span of time. Table 2.1 indicates the temperature resolution achievable by the instrument for varying lengths and averaging time.

TABLE 2.1: Instruments temperature resolution as suggested by the manufacturer for a sampling resolution of 25cm(single ended)

		Range		
		1km	**5km**	**10km**	
Averaging Time	**5s**	0.18	0.63	4.3	**Temperature**
	60s	0.08	0.26	1.8	**Resolution**
	600s	0.02	0.08	0.6	**(deg C)**

Distributed Temperature Sensing (DTS) based on the Raman backscatter from fiber optic cables has found extensive environmental applications [15][16][12]. DTS units

typically provide raw (Figure 2.1) output of temperature traces that are referenced to a single or double (new system) internal calibration coil.Factors such as connector losses, differential attenuation in the external fiber, equilibrium, typically introduce time-varying errors in space and time. Hence the temperature values are based on default assumptions between the internal reference coil and the sensor monitoring it, while considering the above factors. [16].

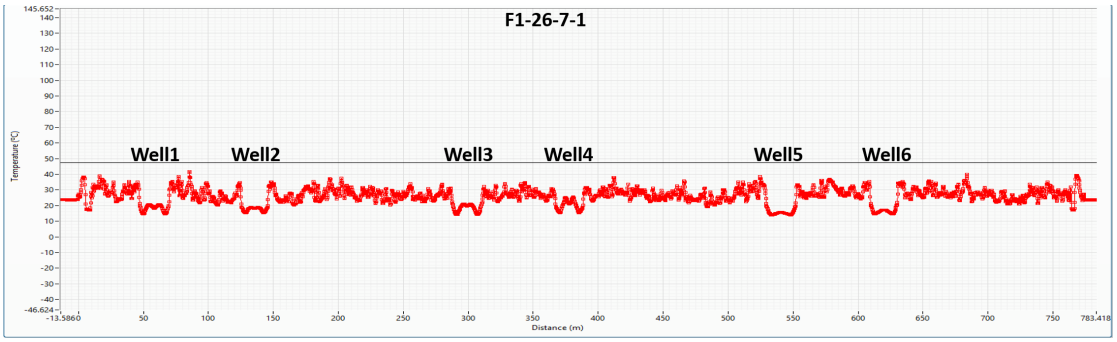

FIGURE 2.1: Labelled screen-Shot of Raw Data from instrument software, indicates symmetric temperature profiles at well locations

These type of losses can however be rectified with the aid of a double ended calibration and water baths. By measuring backscatter from both ends of the fiber optic cable, one can redress the effects of differential attenuation, as caused by bends, splices, and connectors. It can be shown that with double-ended calibration good accuracies can be obtained in the field [17]. Another motivation for double ended measurements is that it allows for direct calculation of the uniform or non-uniform differential attenuation along the cable. Since a field DTS system consists of multiple connections and bends it is necessary to have validation baths along the path to determine with high accuracy the loss experienced by the signal due to an installation. The layout configuration requires extra length of cable to be provided at certain locations as validation baths. The purpose of a validation bath is similar to a calibration bath and would contain water of known temperature monitored with a discreet temperature sensors. After subjection to losses, the fiber optic readings can be validated by the sensors and as a result one would be able to determine the validity of the measurements. By providing possible locations for a validation bath, we provide a means for further calibration of the temperature signal. Double ended configurations have been proven to be more accurate than the instrument-calibrated data, achieving accuracies in the order of tenths of a degree root mean square error (RMSE) and mean bias [17]. For this reason the network is set up to form a closed loop configuration.

2.3 Factors affecting the measured signal and methods for calibration

The instrument provides a graph (Figure 2.2) of the raw signals for the current measurement. There are two plots on the graph, one for Stokes and one for anti-Stokes. The amplitude of the signal is plotted on the Y axis and the distance is plotted on the X axis. This view can be used to examine the signal quality and look for bad splices or connections in the optic fibre that might result in signal loss. A poor splicing would result in step losses and abrupt changes in the signal (anti-Stokes and Stokes).This was not so easily noticed on the field (possibly due to high quality of splice fusion) but theory suggests certain characteristics of the signal can help point towards the possible location of a bad splice.

In the case of double ended measurements it can also be used to check, if the configuration is connected correctly, such that the forward and reverse signals align properly. It can be clearly observed that the signal experiences a loss in power as it propagates the length. Further lengthening of the network would lead to higher attenuation losses which would require a higher number of baths to be installed.

FIGURE 2.2: Screen-shot of Signal amplitude ratios vs Distance for both forward and reverse signals from instrument software, Software also indicates the amount of attenuation loss experienced by fiber

The temperature resolution depends on the measurement time and the launch pulse repetition rate. The laser pulse energy and duration are accurately controlled by the

instrument and optimized at the measurement length to provide the best available temperature resolution performance within acceptable accuracy limits. Longer measurement times can provide temperature readings at a high resolution and can be attributed to the higher averaging time available for the instrument.
Furthermore, shorter acquisition times provide a better view of rapidly changing temperature signatures, but at the cost of higher noise levels. The signal to noise ratio improves approximately as the square root of the acquisition time.The measurement time of the instrument refers to the duration for which the instrument averages the temperature readings plus the time required to generate . The lowest averaging time that can be selected is 5s and highest resolution can be obtained using the 600s averaging time. During a double ended measurement the readings are averaged along both the channels they are connected to resulting in a doubled measurement time.
They are different modes or setting available for calibration within the instruments software. Calibration can be performed with reference sections when the user is able to place one of the two external temperature probes supplied with the XT-DTS in a position such that it is at the same temperature as the average temperature along a section of fibre. The reference section may also be used to calibrate for the temperature offset and fibre differential loss. In the case of the differential loss being calibrated in this way, this option is only accurate if the reference section is in the most distant two-thirds (2/3) of the fibre length. This means, in practice, that the external probe option is generally only used when the end of the fibre returns to a position very close to the XT-DTS unit. In practice, it is normally more effective to calibrate for differential loss using another technique.
Calibration can also be done with a fixed value. Then, the user enters a value into the Fixed Differential Loss field. This should be the difference in the (one way) attenuation experienced between the Stokes (S) and anti-Stokes (aS) signals expressed in dB/km. This can be noticed in the Stokes/Anti-stokes graph and difference of 0.15 dB/km. Usually the optimum setting can be found by ensuring points along the trace which are known to have the same temperature line up correctly (like a calibration bath). If no such points exist, then the default value of 0.255dB/km should be used. This value is the expected value for Corning ClearCurveTM OM3 fibre(Appendix A).
When the user has access to both ends of the fibre a double ended configuration can be set up. The technique works by measuring the signal from both ends of the fibre and using a combination of the signals collected to determine the temperature at all points along the fibre. Double Ended calibration uniquely corrects for a non-uniform differential loss; that is a differential loss that varies over the length of the fibre. The double ended technique is proved to be efficient in a particularly harsh environment where it may be subject to damage-induced differential loss changes. This type of configuration has been chosen for our field and specifics can be found in the upcoming chapter.

Chapter 3

Materials and Methods

This chapter focuses on the field layout and general characteristics of the field experiment conducted. Three pilot locations have been selected for full field scale experiments in the Netherlands, each with a unique fiber optic cable layout. The alignment of configuration was based on drilling locations of wells in an aeration system, such that cable laid on surface met the landfill authorities safety requirements. Further to setting up, the system was calibrated and data collected was analyzed to determine the optimum configuration settings required for the project.

3.1 Site Characteristics

All pilot locations have a bottom liner, a leachate drainage system, a gas drainage system with gas collectors and settlement beacons. The field is divided into compartments that have an area of approximately 2.5 hectares in Wieringermeer and 4.2 hectares at Braambergen. The waste compartments are covered with a layer of soil of thickness varying from 1 to 4.0 m. The soil cover thickness varies and is not uniform along the entire field and is considered to be made of sand. Vegetation in the form of grass exists on top of the soil cover. The height of the waste bodies is between 12-16 m.

3.2 Field layout

The pilots at Braambergen (BB11n and BB11z) and Wieringermeer (W) have been fitted with aeration wells and some of these are equipped with fiber optic cables. (Figure 3.1) shows the final layout to be created such that 12 aeration wells are connected.

Due to time constraints, it was not possible to connect all 12 wells in a field, so a layout of half field was set up. The wells are approximately 10 to 14m deep (length ' c') (Figure 3.2) and have fiber optic cable along the entire depth. The landfill will be eventually fit with optic cable with a net length of almost 2 kilometres. The first phase of installation allowed for 18 wells to be connected across 3 fields. Two of these fields were in the same location (BB11n and BB11z).

Fiber optic cables used for this field research include multi-mode fibers which have as many as 24 fibers per cable. The fibers are well protected with a steel and gel coating to resist installation damages and harsh environments. The high protection available to the fibers make it a time consuming process to create splices and fusions where required. In order to protect the cables on surface, they were installed in HDPE tubes such that they cannot be damaged by mowing machines or animals.

The basic layout of cables (Figure 3.2) consists of a network of cables that begins from the DTS machine ('d') into a calibration bath ('e') followed by connecting wells 1 to 6. Maintaining a network that would follow the already existing pipeline network was of prime importance to avoid damage. The configuration was chosen to be the shortest network that would connect 6 wells and follow pipes. The shortest distance between two wells is depicted by 'a' which ranges from 40 to 50 m at Braambergen (this length is inclusive of the length allotted for a validation bath between two wells, above 5 meters). A longer cable is required to connect the outer wells (2,4,6) to the next well such that the cables follow the pipeline network. This long cable is depicted by 'b' and ranges from 100 to 130m. Wieringermeer is also set up with a similar network with approximately a=45m , b=65m , c=12m. Once the cables are connected, such that all 6 wells form a network, the cable is run back into the calibration bath and then finally back into the DTS machine where it would complete its double ended configuration.

The total network of cables was about 770m in Braambergen 1, 640 in Braambergen 2 and 540 in Wieringermeer. Each well is lined with about 30 meters of cable and about 2 m of wire is protruding out of the well leaving about 28 m of cable within the landfill.(Note: these lengths may vary based on any sort of errors that may have been introduced while installation and can be corrected using a double ended configuration).

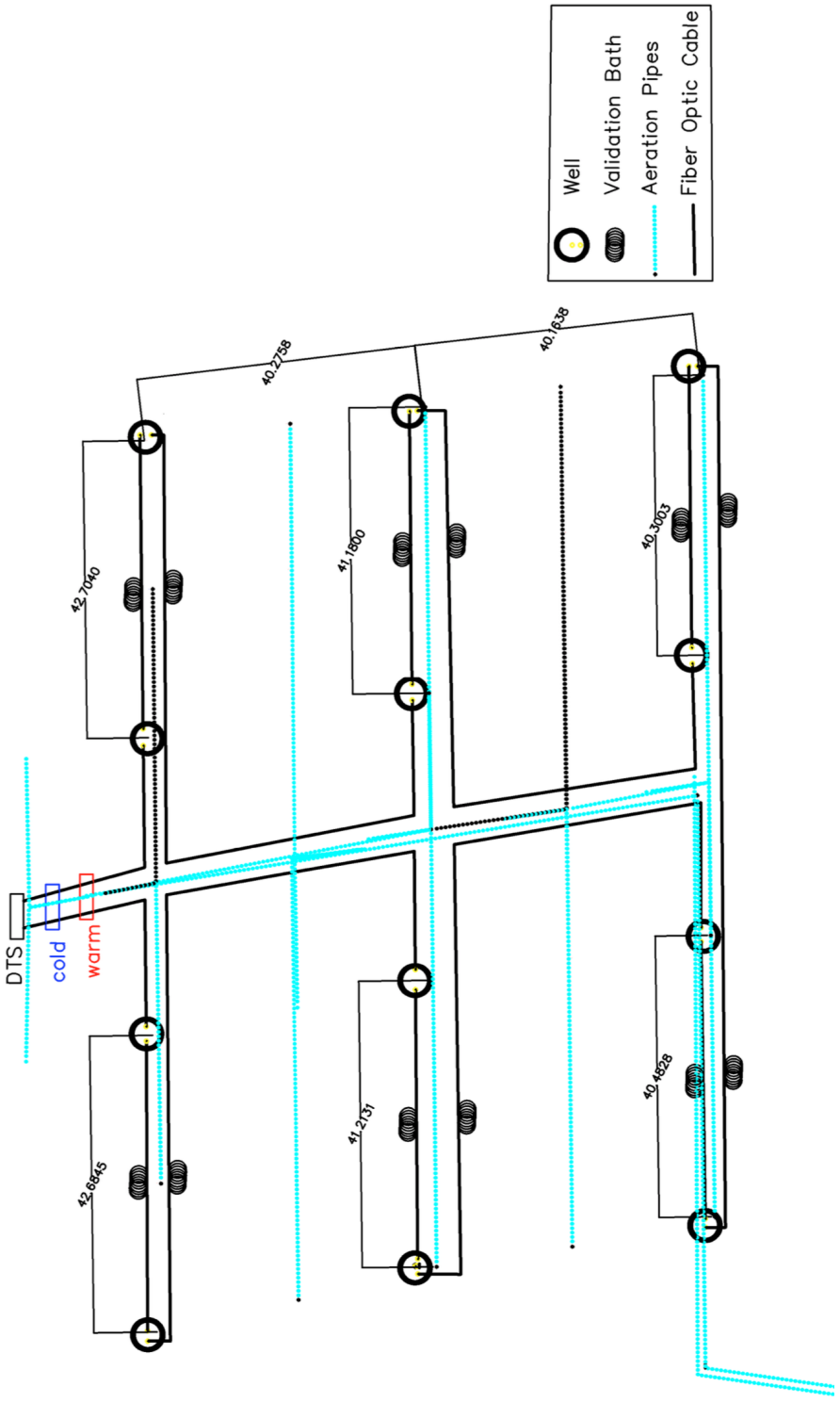

FIGURE 3.1: Braambergen Double ended configuration fibre optic cable layout: The distance between the wells are indicated and the location of baths. The dotted lines represent the existing aeration piping network

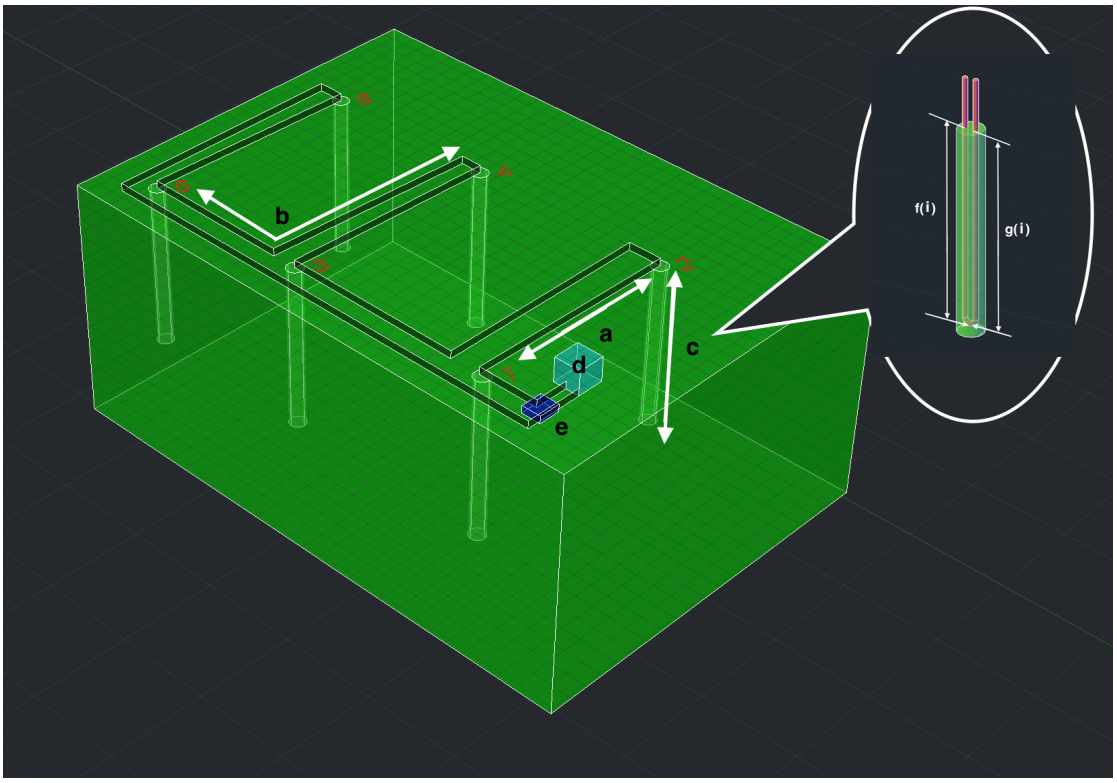

FIGURE 3.2: General three dimensional fibre optic cable layout used for baseline measurements with 6 wells.a and b- length of single piece of FOC, c-Length of installed fiber within well,d-DTS system,e-Calibration bath,f(i) and g(i) are functions holding the temperatures along the cable

3.3 Double Ended configuration

A double ended configuration is required to reduce errors associated with field installations. Quite often the exact length of cable is hard to determine while installing in the field. By using a double ended configuration the user is able to match the forward and reverse signal such that a more accurate reading is obtained and the exact length of the network can be determined. A double ended configuration was set up in the field for its higher performance during field measurements.

A simple calibration bath set up was used on field to check if the instrument could achieve the temperature resolution required along with the double ended configuration. Literature [18] suggested that a length of at least 10 times the spatial resolution be used in the calibration bath, to account for attenuation errors. The bath was therefore a 700x370x220mm Styrofoam box fitted with two frames to be able to coil at least 5 m of cable each. One for the cable starting from the instrument and the other for the cable returning to the instrument. Reference measurements were done in the calibration baths during readings and can be used to compare with cable readings.

3.4 Processing and Analysis Criteria

Mechanical issues might affect the proper depth correlation between the fiber and true depth in the well. One such issue, relates to the fiber optic line coiling up within the well through which it is installed. Such a difference in length can amount to as much as 3 per cent, i.e., the fiber length is 3 per cent longer than the well within which it rests [7]. Mathematically, the difference, is defined as the excess of the fiber length over the tube length. This can be quite easily noticed in the presented observations if one were to have a closer look.

For the requirements of a landfill where the lengths of the well are in the range of 10 to 13m ,the subsequent error is a small length of 30 to 40 cm, which are higher than the sampling resolution of the instrument. The error therefore can not be easily be noticed when the raw data is plotted. Having a closer look at the data this difference is easily noticed and can induce errors in the temperature readings if depth matching is not done. Measured data is plotted by using the deepest point in the well as a reference. The length of cable on either side of the deepest point is considered for the well, by doing so we obtained two sets of temperature data for the same well. When these two data sets are plotted against depth or using a color scheme, the data sets wont align over each other if it is not properly depth matched. For a simple analysis purpose the average of the two data sets were taken to achieve a more rounded observation in this research.

The second issue is a temperature drift caused by the heating up of the DTS instrument. It has been noticed that the instrument tends to heat upon use in the field, this increase in the instruments temperature can cause a drift in temperature readings. This is caused by the relative heating of the reference coils within the instrument. A calibration bath is able to provide an insight of such inconsistencies and a simple error analysis can be carried out with respect to internal reference coil to quantify the changes.

3.4.1 Data Processing

In order to convert the raw data signal into a programmable format, a script from "ctemps.org" was used to convert the raw data signals into '.mat' file. The raw data output provides temperature readings along the length of the cable, it is also compiles raw signals such as Stokes and anti-Stokes readings, reference probe temperatures into a single file.

In order to get an understanding of the obtained temperature readings, we developed a script to visualize the temperature readings in space. Two approaches have been undertaken in order to better visualize the temperatures. One to represent temperature

as a function of depth, each individual data point is represented in a temperature vs length line graph. Secondly, a script that takes temperature readings and associates itself to a certain color, depicting a certain temperature. Both these methods provide insight into temperature changes and trends at different locations. Since the locations and cable lengths remain constant it was required to write a code just once for analysis purposes.

The base criteria for depth matching is to determine the the point of symmetry within a wells temperature profile. The two temperatures sets within the well are a result of the 'U' profile (Figure 3.2) of the cables installed and that temperature would read the same along both lengths. A depth matching technique is used to create the data set, by setting the start of the set from the deepest point within the well. Quite often for analyses the average of the two readings $f(i)$ and$g(i)$ were taken to create a smoother gradient along the depth and to confirm weather the deepest point($f(1) = g(1)$) of the well has been correctly chosen. Here the function $f(i)$ and $g(i)$ represent the temperatures left and right of the deepest point within the well. The initial approximate index value(i) of the deepest point was obtained by simple visual observation of the raw data file.

$$i = Distance\_along\_cable/Sample\_Interval \tag{3.1}$$

For this analysis the smallest sample interval value of 0.254m was chosen. Subsequently if the length of the well is set to be d, the two data sets from within the well would be $f(i)$ and $g(i)$ with n data points. Where i may take value from 1 to n where 1 refers to index value at the deepest point and n at the prescribed depth. The value of i is correctly selected if the average error($error_{\text{avg}}$) i.e.

$$error_{avg} = Mean|f(i) - g(i)| \tag{3.2}$$

is minimized . In figure(3.3) we show the average error for 6 consecutive index values, where the point of symmetry was around the distance of 39m. The results clearly indicate the minimum error is for index value 154. Hence, it can be assumed to be the deepest point within this particular well is at a distance of 39.116m. This criterium is applied at all well locations to determine the deepest point within the wells.

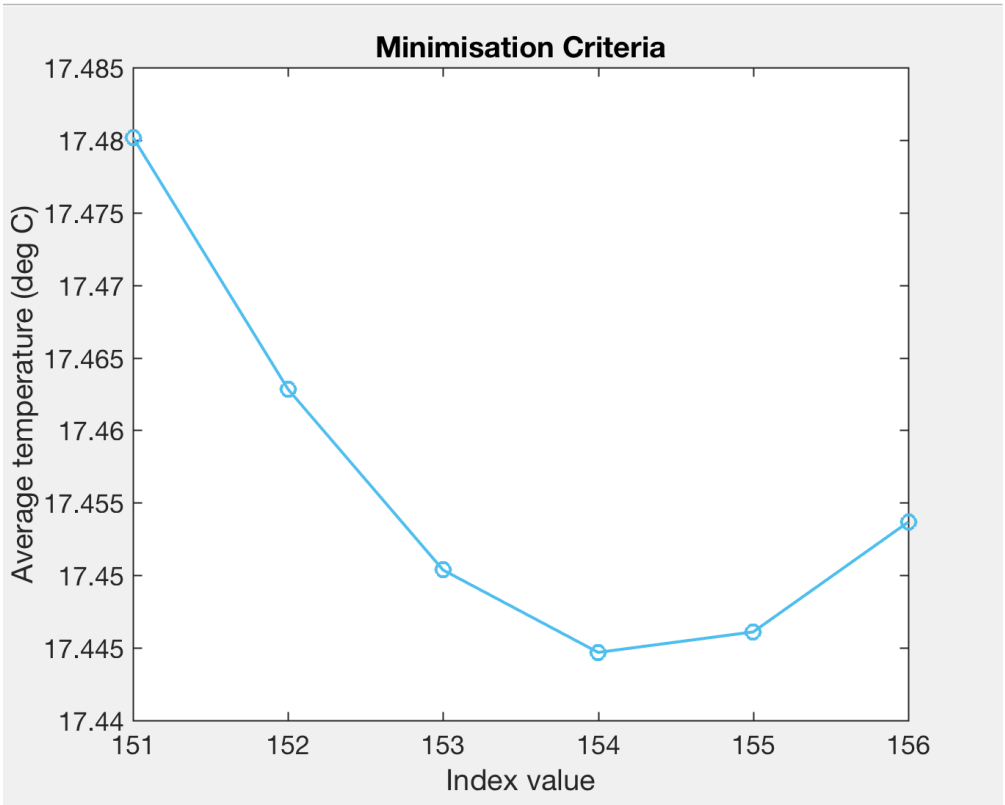

FIGURE 3.3: Results of minimization criteria for depth matching indicates the index value for which the average error is minimum

Once the point of symmetry is correctly estimated an uncertainty analysis is carried out. By doing so it was able to determine the fluctuations in temperature readings in space and time.Standard deviation and mean of temperature differences are used to determine by how much the temperature readings deviates from the true value.This analysis would enable us to address the repeatability and resolution of the system.

3.5 Instrument Response

The system allows the user to set acquisition time(AT) from a minimum of 10 seconds per measurement to as much as 20 min per measurement in a double ended configuration. Longer acquisition time is ideal to be used when high temporal resolutions are required whereas shorter acquisition times are ideal to notice quick or abrupt changes within the system. The effect of higher AT on accuracy can be noticed in the graph below(Figure 3.4). It can be seen that a higher AT results in more accurate values in comparison with a discreet PT-100 probe. The calibration bath is ideally located close

to the instrument location such that the cable leaving and returning(forward and reverse) to the system can be analyzed for errors induced due to loses.

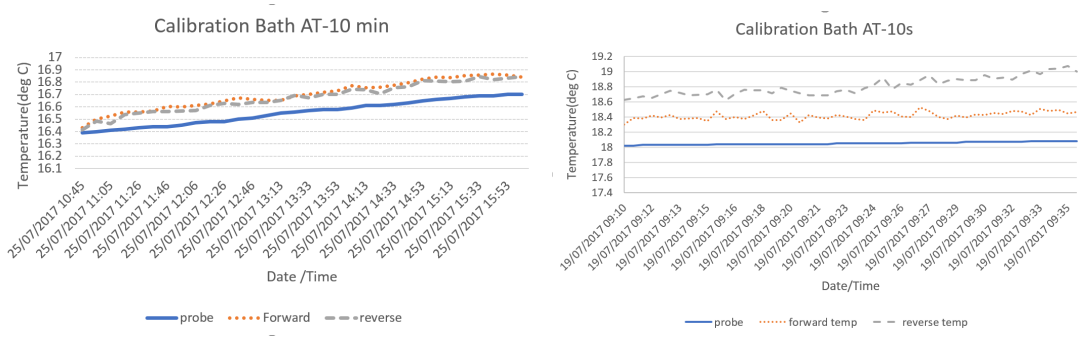

FIGURE 3.4: Callibration Bath Readings AT=10min(left), AT=10s(right) indicate higher accuracy readings with higher AT

Initial field tests suggested that a maximum acquisition time be used to monitor the field data for mainly two reasons. Firstly, the temperatures within the wells remain relatively constant over hours during the day and moreover literature suggested temperature changes within a landfill occur at a very slow rate such that it can be quite easily noticed even with a higher acquisition time. Secondly, using high acquisition times would lead to generation of less data points in time and reduce processing time of the raw signal.

A typical system is characterized by the spatial and temperature resolution. The spatial resolution, is the minimum distance of the sensor to measure a step change in temperature along the optical fibre(for this case 0.254m). The temperature resolution is a measure of the precision to distinguish the absolute temperature(as high as 0.02 deg C). The temperature resolution depends on the measurement time and the launch pulse repetition rate [19].

3.5.1 Infiltration experiment

In order to simulate a precipitation like event that would result in changes of temperature within the well, a high volume precipitation event was artificially induced by pouring water directly on top of the well. The basic idea of this was to check if the instrument detected temperature changes during the water pouring duration. In this experiment a water can of capacity 35 liters was emptied by a constant head tap. The water temperature and duration of the pouring event was recorded to be between 19 and 23 deg C for 7.5 minutes. Since machine response had to be computed the test was carried out using the same volume and temperature range of water but with different acquisition times.

3.5.2 Uncertainity Analysis

Higher AT leads to less uncertain temperature readings or high accuracy readings. The above test were able to provide insight into the reliability of the obtained readings. Further an analysis is carried out between the two data sets$f(i)$ and $g(i)$ to check for variation of temperature in time. The difference in temperature readings at the same depth at two different points in the cable are expected to stay relatively constant inside the soil. For example, if the length of the well to be analyzed is 10m and a spatial resolution of 0.25cm is selected, there should be 40 data points from the deepest point of the well. $f(1) = g(1)$ equals the temperature at point of symmetry of temperature profile $f(40)$ and $g(40)$ would represent the temperatures at top of 10m. In the terms of time, the measurement would repeat according to the set acquisition time which generates a data set in time.

The difference in temperature ($A_{i,t}$) at a particular index value at time 't' is calculated as the difference

$$A_{i,t} = f(i,t) - g(i,t) \tag{3.3}$$

Larger the difference of $A_{i,t}$ indicates that higher errors in readings are induced. Errors in the DTS readings can be associated to non symmetric installation of cables into wells or due to bad splicing and bends within the network. Splices and bends can be corrected by using the provided baths, but determining the exact length of cable inside the ground requires more than a minimization criteria.

3.5.3 Depth Matching

As suggested earlier depth matching is required to correct the temperature readings with respect to its correct position in space. The readings obtained along the two lengths of fibers within the well have to be matched.
The depth matching algorithm considers the index value from the minimization criteria and then optimizes the sampling distance to account for the coiling of cable inside the well. The algorithm:

- Step 1: Select the point of symmetry of temperature profile using minimization criteria.
- Step 2: Create a data set of positions in depth wrt point of symmetry for cable entering the well($z1$) and cable leaving the well($z2$), using a variable sample interval($sd1$ and $sd2$).

- Step 3: Use obtained readings of first length to create a spline function(T1tst) of temperature readings in depth using 1D interpolation.
- Step 4: Repeat Step 3 for second length of cable within well, thereby creating a second spline functions($T2tst$) that describe the temperature readings at specified positions from Step 2.
- Step 5: The main objective here is to reduce the error in the position of temperature readings. This can be done by minimizing the value of $\sqrt{(T1tst)^2 - (T2tst)^2}$.
- Step 6: Using 'fminsearch' function from Matlab it is possible to find the smallest value for $sd1$ and $sd2$ that would result to a minimum value of the objective function from Step 5.
- Step 7: Use results from Step 6 to determine the change of sampling interval.

The above algorithm attempts to match temperature to depth found inside a well by optimizing the sampling interval along both lengths within the well. It is also possible to do the same by just optimizing only one of the sampling intervals and keeping the other constant.

3.6 Baseline measurement

The basic motive of taking a baseline measurement is to observe temperatures within the landfill during its anaerobic decomposition phase before aeration treatment. By doing so, one can compare it to any change associated with aeration at a later phase of the project.

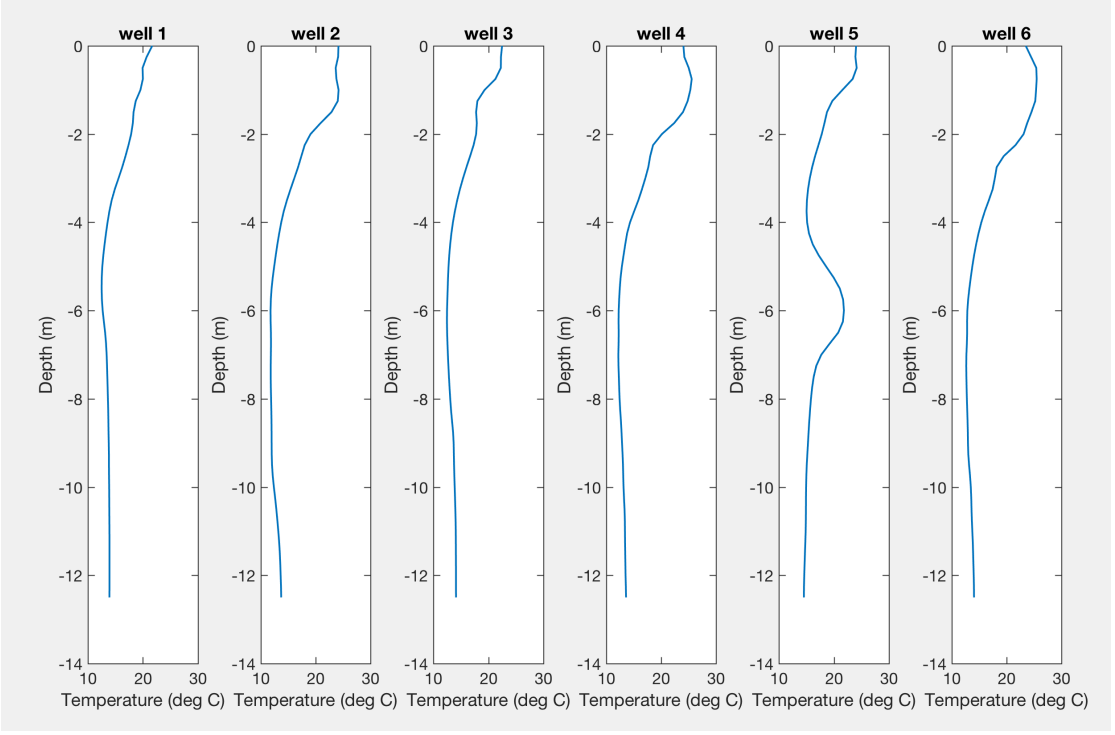

FIGURE 3.5: B11z_250717_B1_6 Well temperatures along depth (0=ground level), indicate less variation in depth

The results were recorded over depth at a certain instance in time (Figure 3.5). It was noticed that the temperature along the depth of the well did not vary much as we move deeper into the soil. The baseline measurements were carried out from 19th to 26th July 2017. The surface temperatures are recorded to be much higher than the ground temperature. A short summary of tests carried out is present in (Table 3.1). Each test has been given a unique serial number. The basic format of the serial number is Test Location_Date_Test Type_Number of wells. The test have been organized chronologically, in which F, B, A represents 'First', 'Baseline' and 'Aeration' respectively. The remarks beside some test details indicate certain observations during the test. These include first installation of validation bath, determining entry point of cables in to wells, damaged readings etc.

TABLE 3.1: Test Details

Instrument Model	SilixaXT-DTS	**Fiber optic cable**	SLT STA with E glass	**Total Fiber Optic length**	BB11n-760m BB11z-630m W-545m Total-1.935m	
S.no	**Acquisition Time (s)**	**Date (2017)**	**Start time**	**End Time**	**Duration (hrs)**	**Remarks**
BB11n_130617_F1_2	300	13-Jun	12:28	12:38	00:10	
BB11n_140617_F1_2	10	14-Jun	14:35	17:15	02:40	
BB11n_100717_F1_6	10	10-Jul	14:01	15:12	01:11	Introduction of calibration bath
BB11n_100717_F2_6	300	10-Jul	15:34	16:04	00:30	
BB11n_100717_F3_6	30	10-Jul	16:13	16:21	00:08	
BB11z_140717_F1_5	30	14-Jul	14:42	15:32	00:50	Cable network damaged due to strong winds
BB11z_140717_F2_5	60	14-Jul	09:47	11:59	02:12	
BB11z_140717_F3_5	10	14-Jul	12:01	14:11	02:10	Ice pack used to determine well entry points
BB11n_190717_B1_6	10	19-Jul	09:10	09:49	00:39	
BB11n_190717_B2_6	300	19-Jul	11:19	11:59	00:40	
BB11z_190717_B-6	300	19-Jul	12:37	15:48	03:11	
W_200717_B1_6	300	20-Jul	10:44	15:26	04:42	
W_200717_B2_6	60	20-Jul	15:29	16:09	00:40	
W_200717_B3_6	10	20-Jul	16:18	17:22	01:04	Infiltration experiment at well 4
W_240717_B1_6	300	24-Jul	09:26	16:40	07:14	
W_240717_B2_6	10	24-Jul	16:45	18:05	01:20	Infiltration experiment at well 3
BB11z_250717_B1_6	300	25-Jul	10:45	16:03	05:18	Infiltration experiment at well 5
BB11z_250717_B2_6	10	25-Jul	16:09	16:55	00:46	Infiltration experiment at well 5
BB11n_260717_B1_6	300	26-Jul	10:58	15:59	05:01	Infiltration experiment well 2
BB11n_080917_A1_6	1200	08-Sep	10:07	11:48	01:41	Aeration begins (10am)
BB11n_080917_A2_6	600	08-Sep	12:13	16:24	04:11	

Chapter 4

Results and Discussion

4.1 First Tests

The first field test included temperature readings from two wells at the Braambergen landfill. The test was carried out to just get an initial idea of the temperatures within the landfill and what settings configuration would be ideal once rest of the wells were connected. The test readings of temperature recorded are higher than the surface (30 to 40 deg C) in comparison to the waste body (15 to 20 deg C). On a sunny day the black fibre optic cables tend to heat up to a much higher temperature than the air temperature around. The readings on surface are not representative of the actual air temperature but provide an insight into the variation of temperature over time. Along the depth of the landfill, the temperature fluctuations are not much and appear constant relative to the surface. The test duration was almost 2 hours and 40 minutes with just two wells connected. Figure 4.1 is a line graph showing the variation of temperature in time with the aid of multiple lines. Other observations include that, the surface temperature fluctuates much more than inside the well, resulting in the narrow profile at depths below 0.

The effect of precipitation was thought to be the easiest to notice in this network of sensors. The sudden and cyclic changes in temperatures due to random long and short spells of rain is captured on the surface, while the well temperature remained somewhat constant. Further, it was hard to notice within the well the effect of precipitation considering the short duration of rain events and short test periods.

After the first test on the field with two wells, the fields of Braambergen (BB_{big} and BB_{small}) and Wieringermeer (W) were connected with six wells each, resulting in a total of 18 wells. Further allowing for a baseline measurement to be carried out for 39 hours in total. The breakdown of various tests are presented in table 3.1.

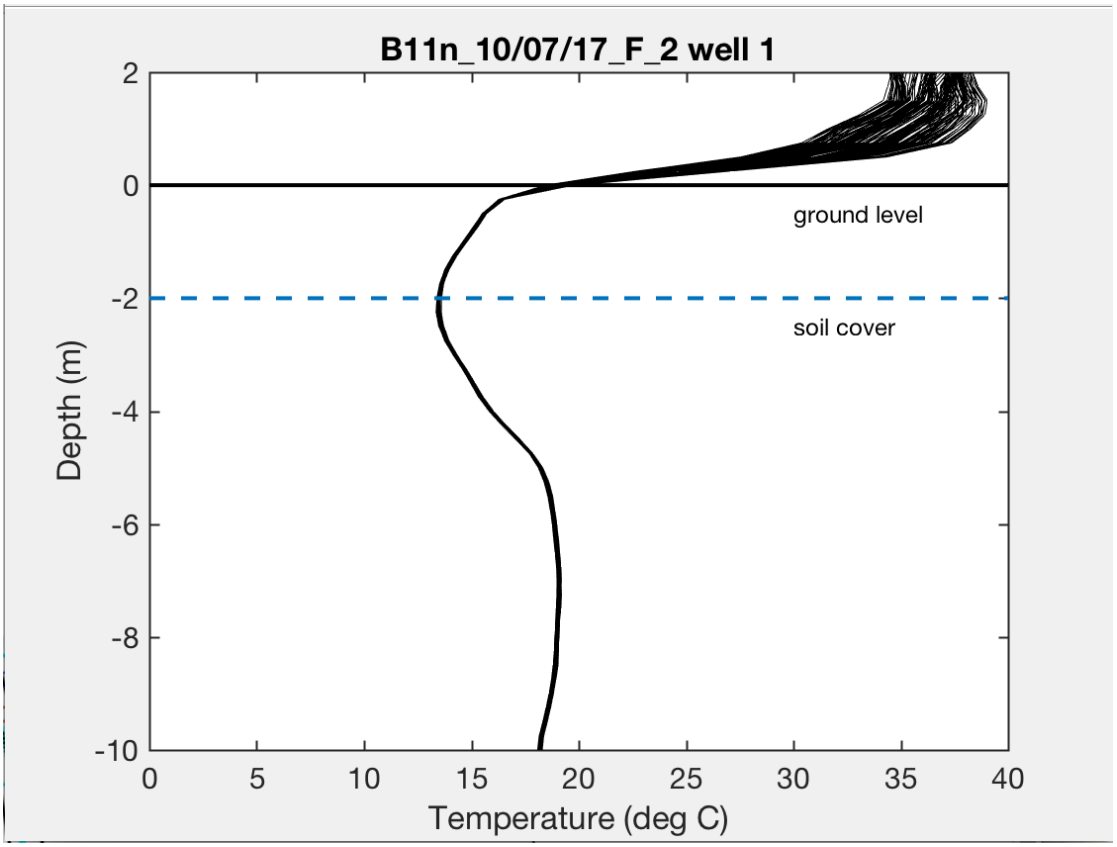

FIGURE 4.1: Well and Surface temperature for a single well at Location:BB11n indicates the high variation of surface temperature compared to the temperatures within the well for a test duration of 2 hours 40 minutes

4.1.1 Response to water infiltration

Observing the minimum and maximum values of temperature within the well over time (at -2.5 and -10 m depth in figure 4.1), it can be quite clearly seen that they stay relatively constant over a single test period. A water pouring experiment was carried out to understand the response of the machine to temperature changes during a single test period. Following relatively constant temperatures within the well, the maximum and minimum temperature occurred at two distinctive depths (figure 4.2, o and x markers). The minimum was often noticed right below the soil cover whereas the maximum was seen more buried in the waste. It was logical then to expect the maximum and minimum temperatures within the well to change when water of higher temperature was poured into them.

From the water pouring experiments results it can quite clearly be seen in figure 4.2, that the 10 second acquisition time event provided a higher resolution of the temperature increase and decrease within the well with respect to time. It can also be observed that the increase in temperature at Braambergen is slower than at Wieringermeer. This is likely caused by a lower permeability as a result of higher compaction around the well.

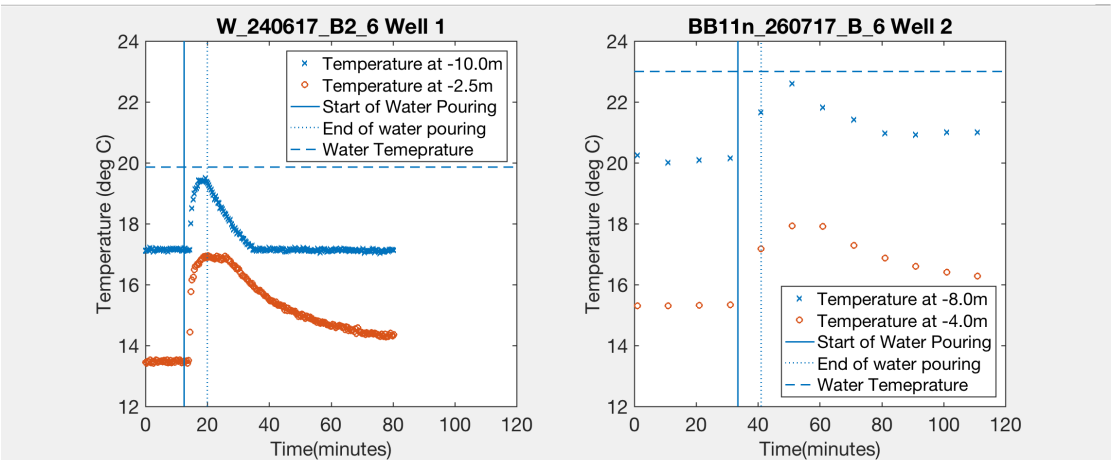

FIGURE 4.2: Instrument response to water pouring experiment using different acquisition time, 10s AT(left) 10min AT(right)

The vertical lines in the graph represent the start(solid) and end(dot) of pouring respectively and the horizontal dashed line indicates the temperature of the water poured. Increasing AT may have resulted in loss of temporal detail but it provides an increase in measurement accuracy which can be seen in inferred from the calibration bath readings and subsection validity of the measurements, error analysis.

The above result suggests that monitoring a process that is quick like for example sudden heavy rain or quick fires is better captured with a short acquisition time. Whereas, for the long run and for slowly heating up or cooling process a higher acquisition time is better. Another benefit of using a higher sampling time is that noise in the temperature signal and number of data points are reduced in time. Where as the lower AT would have a higher temporal detail, i.e a temperature reading approximately every 10 seconds it comes at a price of a lower resolution in temperature.

Another important observation of the water pouring experiment was that the soil waste does not entirely enclose fibre optic cable, this can be attributed to the soil retaining the cylindrical well profile after drilling, which results in some space between the wire and the soil. When water was poured the change in temperature was noticed at depths of 6 to 8 meters almost instantly indicating that the well is much more permeable than the soil itself. Hence, it should be kept in mind that the temperature within the wells could be representative of the air temperature within the well and not purely of the soil itself.

4.1.2 Baseline Readings

Measurements at the eighteen wells show trends in temperature profiles as we move along depth. The temperature profile is generalized into the maximum and minimum temperature within the wells at each location with an indication of the range of surface temperature (table 4.1). The table indicates a minimum temperature which can quite often be noticed in the well profile near the bottom of the soil cover. Whereas the maximum temperature is noticed much deeper inside the waste. What is observed at the deepest point of the well is that the landfill gets warmer as we move deeper by almost 2-4 deg C with respect to the minimum from the soil cover. Since the profiles were not the same it was not possible to determine an exact value for this temperature difference.

TABLE 4.1: Observed temperature range(deg C) summary

	Maximum well Temperature	**Minimum well temperature**	**Surface Temperature**	**Temperature at deepest point**
BB_{big}	18	12	20-28	14
BB_{small}	25	14	25-35	18
W	25	14	20-30	18

This variation of temperatures along the depth can be attributed to the heterogeneous nature of the waste within the landfill. Variation of biological activity has not been quantified but a conceptual model can be formulated using post aeration data.
In order to better understand the ranges of temperatures along the depth of the landfill, the bottom 10 m of the well were observed (figures 4.3, 4.4, 4.5). The bottom 10 m was chosen for the reason that the top few meters where the cable enters the soil cover(dash line) is not completely enclosed, thereby making it less sensitive to temperature fluctuations from the surface. Further, there could be some uncertainties in these values of temperatures which the error analysis would suggest.

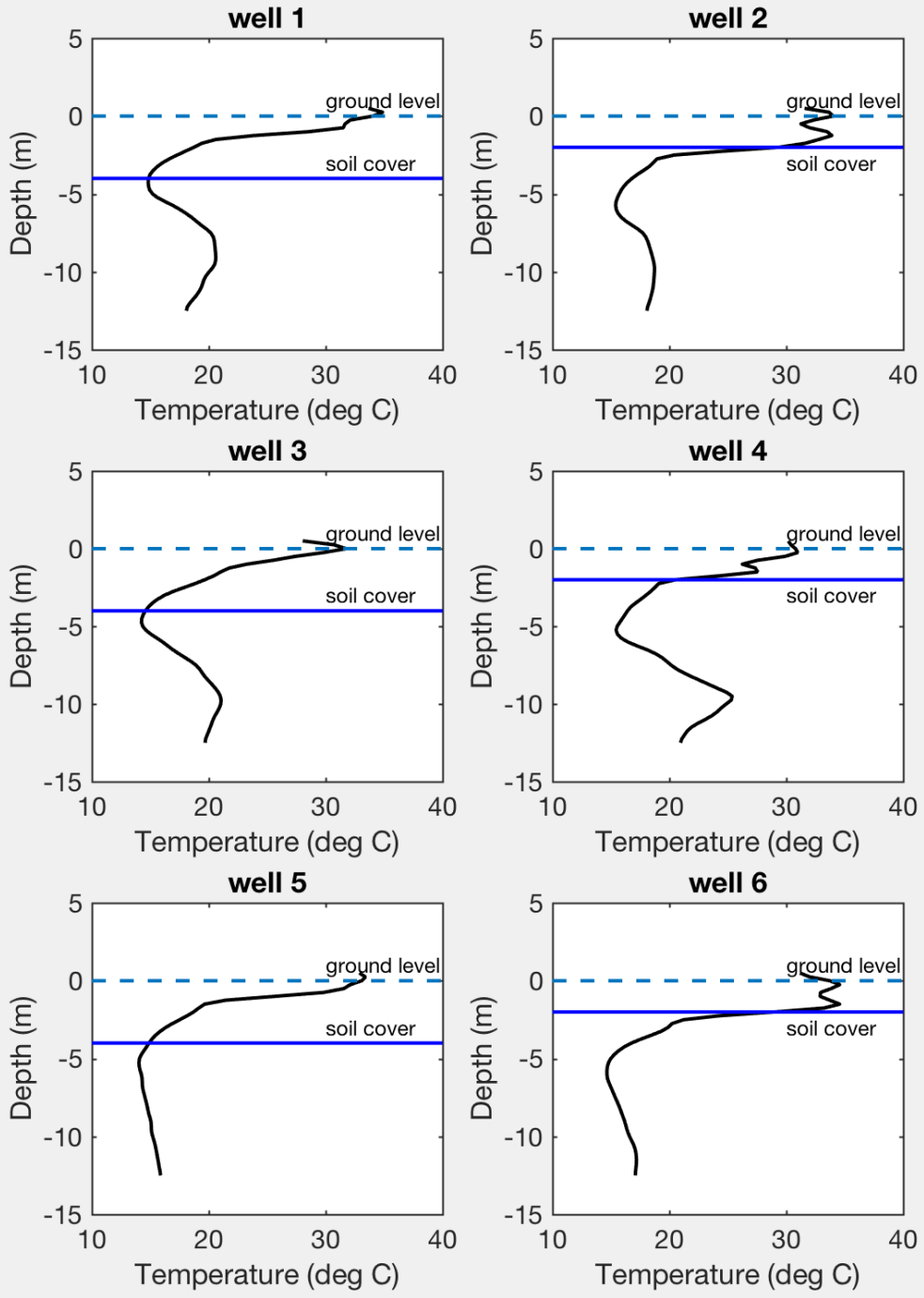

FIGURE 4.3: 'BB11n26/07/17B16' Well Profiles

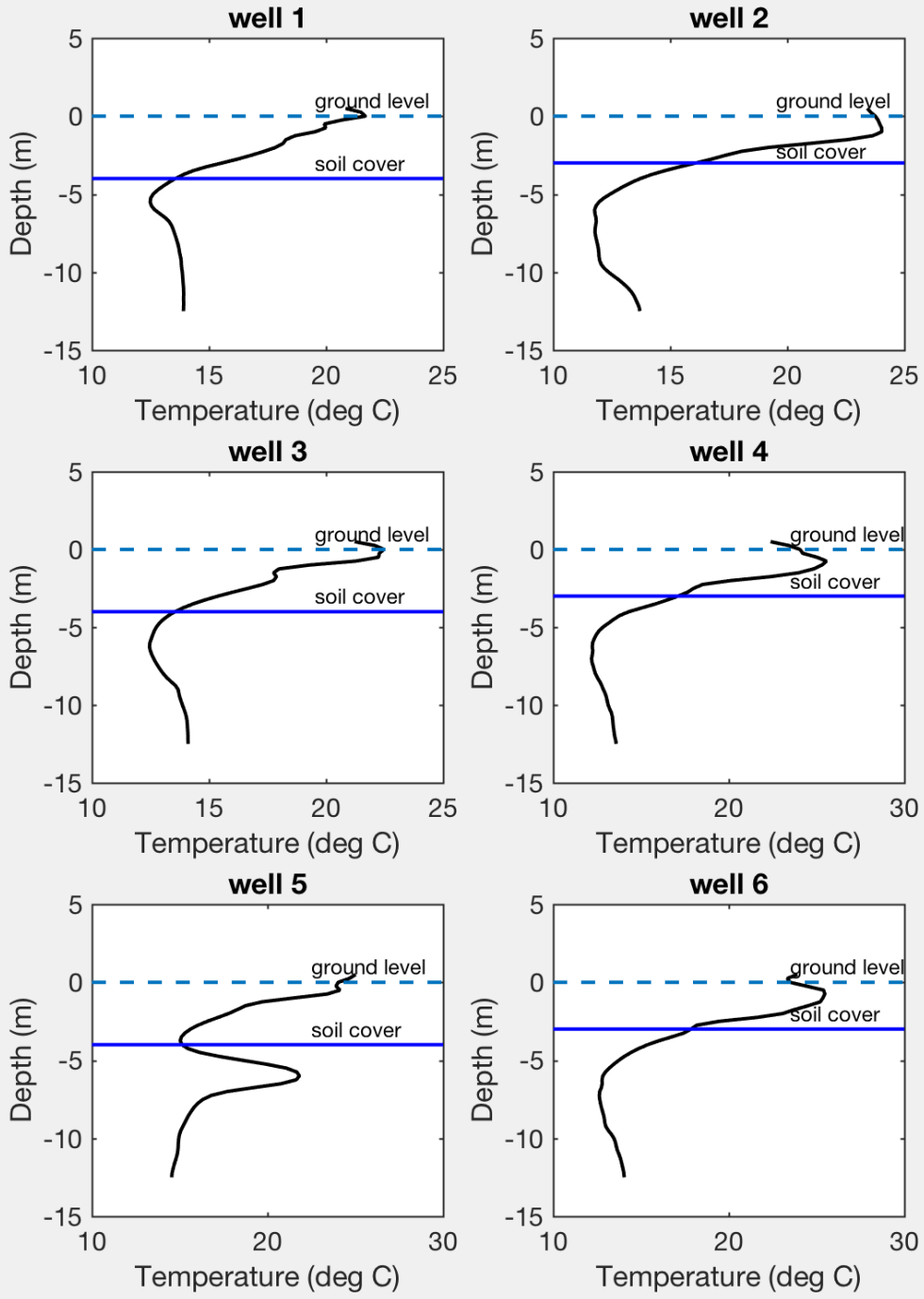

FIGURE 4.4: BB11z25/07/17B16 Well Profiles

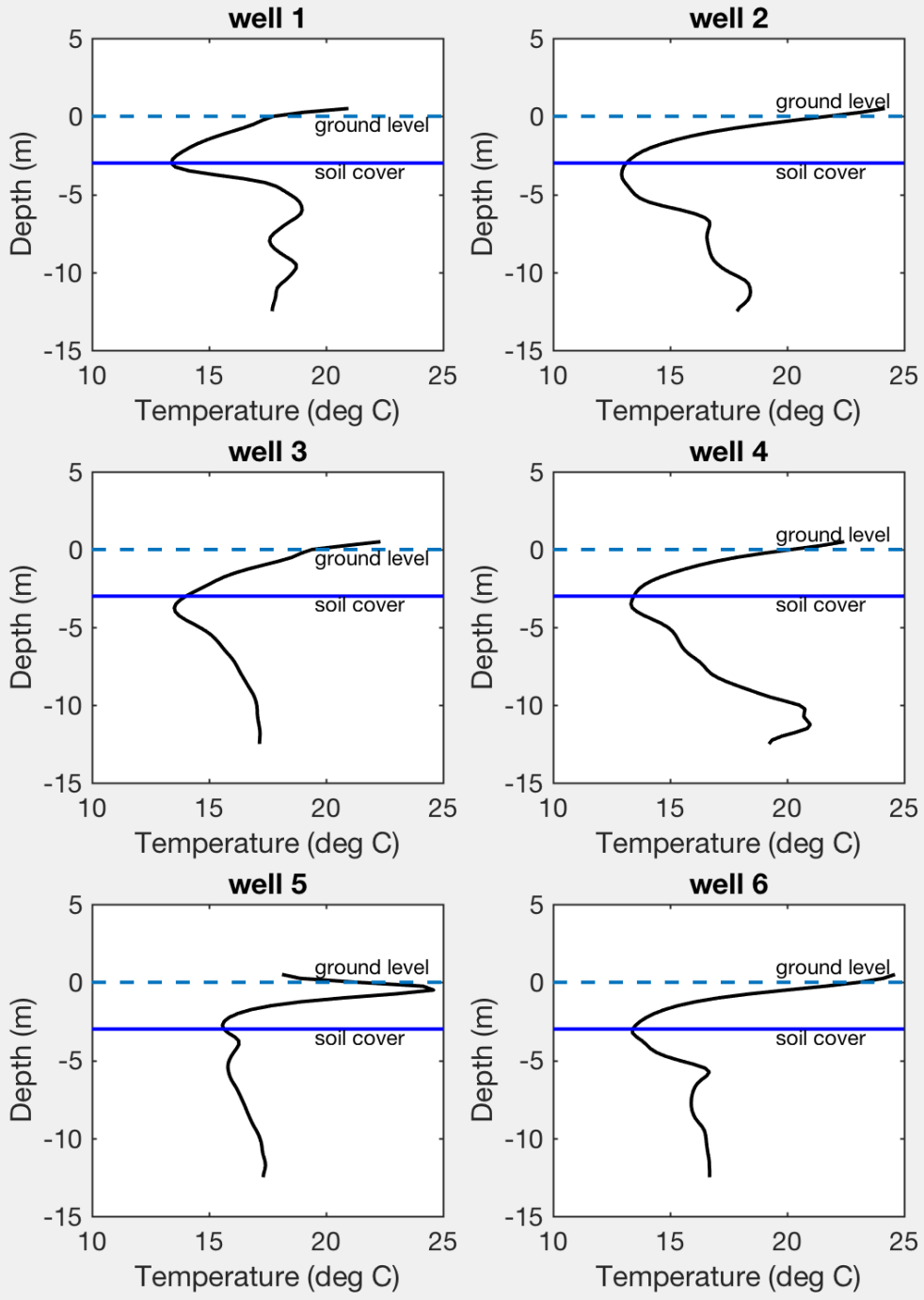

FIGURE 4.5: 'W24/07/17B16' Well Profiles

Variation of temperature as the cable entered the well is reduced and only natural to find as the cables are shielded from the fluctuation of radiation and precipitation. The profile can be divided into 2 zones namely the soil cover and waste body.
The trend of rise in temperature as we move deeper into the well is similar in all 3 fields and majority of the wells except one: well 5 at BB11z (figure 4.4). The readings have to be compared to post aeration readings to explain the profile. Since this inconsistent trend occurs below the soil cover it could be a region of high biological activity or result of waste heterogeneity.

4.1.3 Validity of the measurements, uncertainty analysis

What can be noticed from the previous section is that all the well temperature profiles with respect to depth have a similar trend. The trend being a decrease with respect to temperature along the length of the soil cover and an increase in temperature as we move deeper into the waste. An uncertainty analysis is required to quantify the fluctuations of temperature readings in time and depth. The field of Wieringermeer was chosen for this analysis.

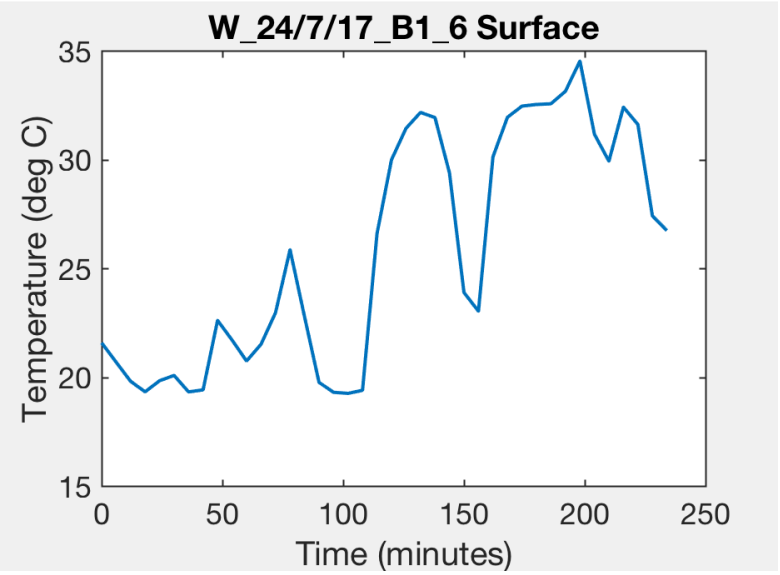

FIGURE 4.6: Surface temperature variation in time, where 0 indicates the start of the test

The readings of surface temperature were plotted for a duration of 4 hours (figure 4.6). The occasional dips in the surface temperature can be attributed to the passing cloud cover. The measurement interval of the surface temperature was 10 min between readings for around 240 minutes. It can be seen that the temperature fluctuated from slightly below 20 deg C to above 30 deg C on the surface. Having stated the resolution that can

be achieved by using higher AT is in the range of 0.02 deg C, it was necessary to analyze if the fluctuation in readings were within the prescribed range.

Uncertainty of the position of the cable inside the well can induce error in readings if proper depth matching is not done. Errors can occur while trying to correctly detect the length of the cable at well locations. The error is assumed as the difference between function $f(x)$ and $g(x)$(3.2) This assumption arises from considering that both $f(x)$ and $g(x)$ are equally spaced in depth. But in reality this may not be the case and the difference between the two functions would be high if not matched properly.

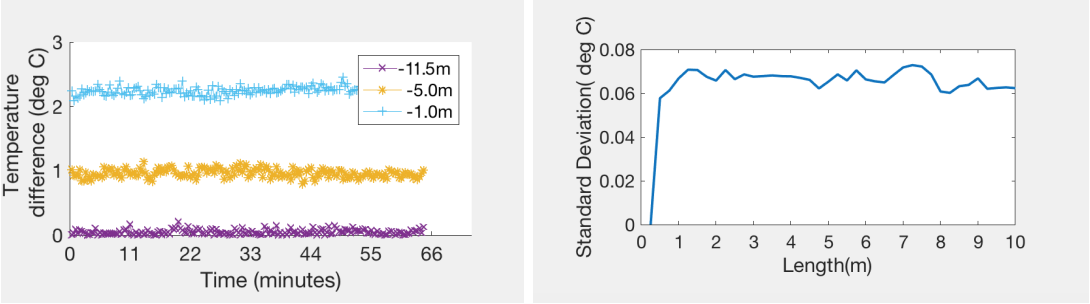

FIGURE 4.7: Temperature difference between cable entering and leaving well 1 at different depths in time. AT=10s,Standard Deviation(right)vs Length, Temperature Difference vs time(left)

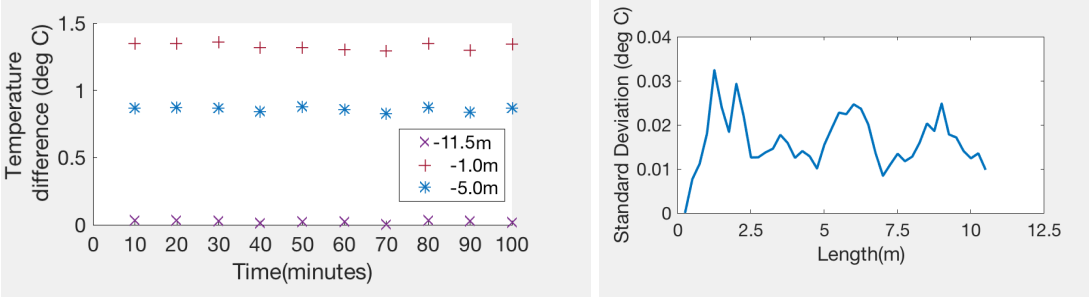

FIGURE 4.8: Temperature difference between cable entering and leaving well 1 at different depths in time. AT=10min,Standard Deviation(right)vs Length, Temperature Difference vs time(left)

Having stated the resolution that can be achieved by using higher AT is in the range of 0.02 deg C, it was also necessary to analyze if the fluctuation in readings were within the prescribed range. The fluctuation of the temperature difference was plotted for the length of a single well and for the duration of the test with two different acquisition times(figure 4.7 and figure 4.8). This investigation led to deeper understanding of the effect of choosing a higher acquisition time. The range of error reduced from 2 to below 1.5 degrees (figure 4.9 and figure 4.10). Since the bottom of the well is set as the starting point of the analysis the standard deviation at the deepest point would indicate a value 0. There is a decrease in error (Figure 4.7, 4.8) by merely increasing the acquisition time (AT). The value of standard deviation is noticed to decrease from 0.06 to 0.02(deg C)

The results of this analysis suggested that the difference is relatively constant over time for each depth as can be seen in (figure 4.7 and figure 4.8(left)). The slight fluctuation of error values in time can be quantified with the help of a standard deviation plot of the error at each depth (figure 4.7 and figure 4.8(right)).

Another observation regarding the fluctuation, is that the difference between the two obtained data sets were higher near the surface of the well. Figure 4.9 is an error bar plot that indicates the variation of error from the mean error at each data point. When compared to the readings of a higher acquisition time(Figure 4.10), it is noticed that the error range decreases.

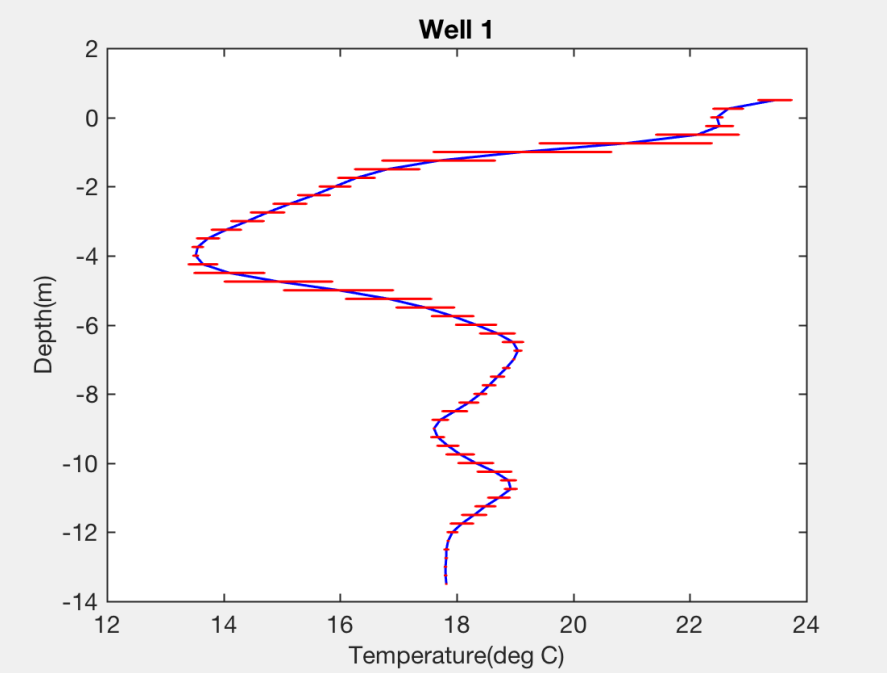

FIGURE 4.9: Error bar plot of Wieringermeer Well Profile 10s AT, indicates high temperature difference along gradients and close to the surface

By analyzing the readings from the 6 wells it can be seen that the difference is 1 to 2.0 deg C, with the higher differences found near the surface. The higher values near the surface could be a result of wrong depth matching. Using the algorithm described in 3.5.3 the high temperature differences can be reduced. The results 4.11 of obtained temperature profile after depth matching has corrected the high errors on the top of the surface, but the errors at the mid locations still are similar to the initial estimation. This result clearly indicated that there is an uncertainty in the position of the optic cable and should be corrected for optimum results.

Two different temperature readings can occur if the distance between the cables within the well are high. These errors can be a result of mainly two reasons, one the temperature fluctuations near the surface is more evident due to the cable not being enclosed

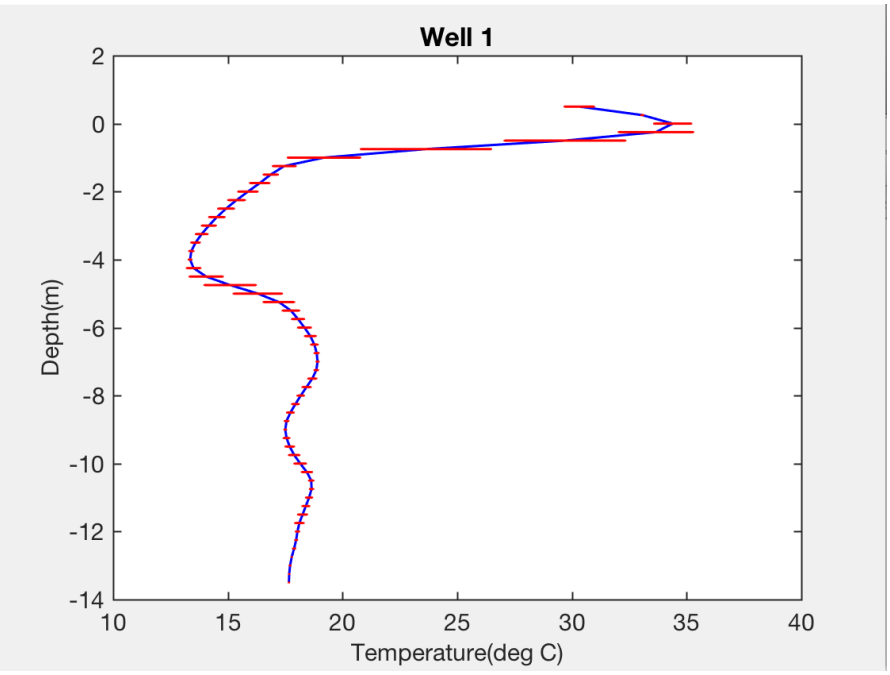

FIGURE 4.10: Error bar plot of Wieringermeer Well Profile 10min AT, indicates lower temperature than 10s

properly(especially near the surface). Secondly, the over-stuff would result in a difference of temperature if the cable is not installed in a perfect 'U' profile.

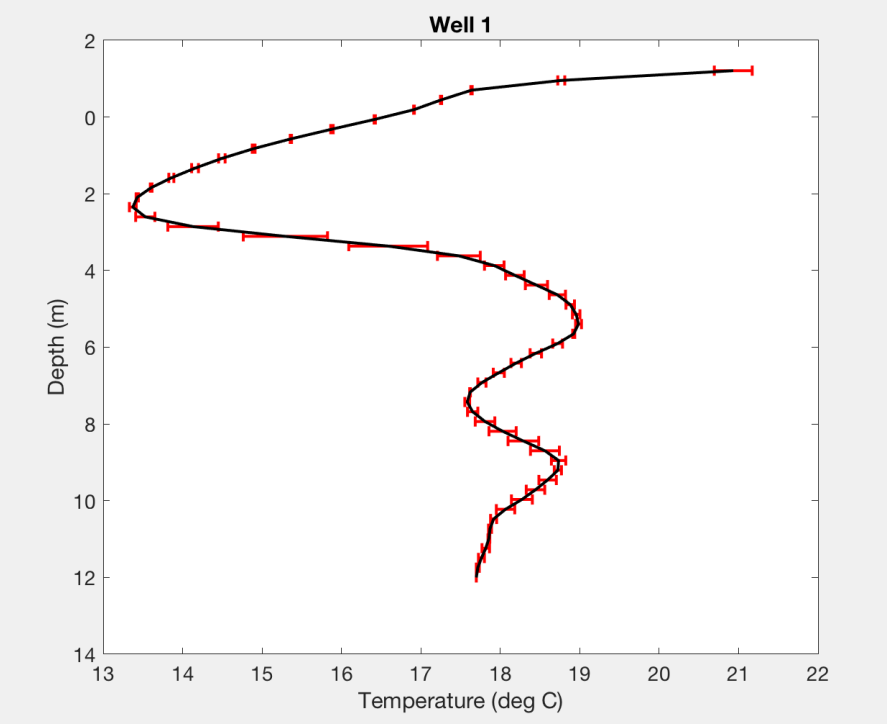

FIGURE 4.11: Error bar plot of Wieringermeer Well after using Depth match algorithm, indicates reduction of error near the surface

The previous analysis provides user with information regarding the reproducibilty of the temperature readings. Accuracy of the instrument was only tested with the aid of a simple validation bath. With the available information now, it is also possible to compare temperature readings to a standard value using other discreet sensors. Using a standard validation baths we can address questions regarding accuracy at high resolutions. By doing so, temperature readings from within the well can be narrowed down to more accurate readings with errors much less than 0.05 deg C.

4.1.4 The Soil Cover

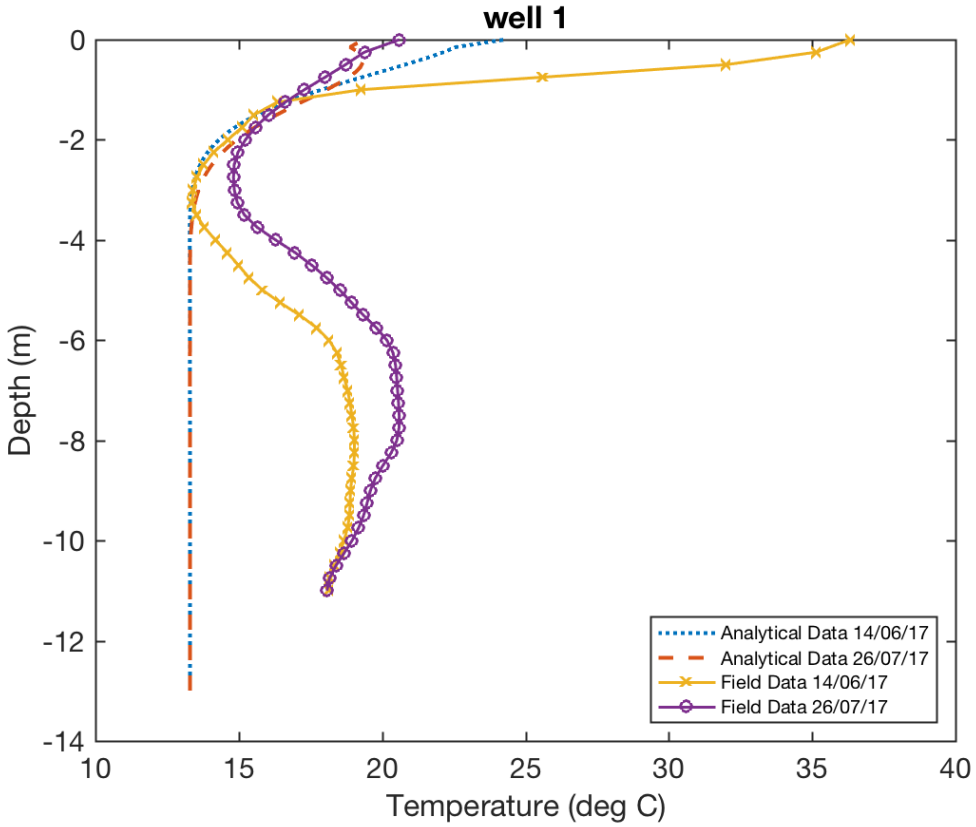

FIGURE 4.12: Well temperatures one month apart with analytical ground temperature

Seasonal variations in surface temperatures can be well captured with the DTS system as shown in figure 4.12 where the 'x' marker represent the test carried out on (14/06/17) and a 'o' marker for the test carried out on (26/07/2017). It can be noticed that the average air temperature is much cooler a month later. However a slightly higher mean well temperature is observed due to the downward diffusion of surface heat. The well retains its temperature profile, a slight decrease in temperature is noticed in the soil cover and subsequently an increase as we move down the waste. This can be attributed

to the change of weather and the onset of rains in the month of June and July in the Netherlands.

Figure 4.12 uses the 1D heat model mentioned in Chapter 2 to predict the ground temperature along the depth of soil. These temperature profiles are indicated by dash and dotted lines. The analytic formulation estimated the surface temperature for the soil cover(upto -3.0m). The temperature formulation takes the following assumptions i.e. the soil has wet bulk density $\rho_{bw} = 2000kg/m^3$ and heat capacity $C_p = 1000J/(kgK)$ cover is made of sand of thermal diffusivity of 0.2 m^2/s for the first 3m and rest of 10m the soil is given a diffusivity value of 0.1 m^2/s. Surface wave amplitude was set at 7.5 deg C, phase constant of 34.6 days with surface temperature at 18 deg C for best fit. The two test was held 42 days apart and the temperatures were plotted for the full length of the well.

Field observation indicate an increase in well temperature as we move deeper than the soil cover. This increase in temperature can be associated to two main reasons. Firstly, the landfill could possibly be generating heat as result of bio-activity. Secondly, the ground temperature increase as we move deeper could be a result of time lag of surface heat. Results from the 1D heat model suggest that the heat from surface is significantly damped as it propagates through the soil cover and attains an equilibrium temperature before reaching the waste.

The analytical profile obtained in Figure 4.12 holds true for the entire depth only if its constituents are made of homogeneous properties as assumed in the formulation. By observing the values obtained at the field and assuming that the waste below is biologically active, it can be seen that the waste below is much hotter than estimated analytically. The lower temperatures here are a direct indication of the waste having a lower value of thermal diffusivity compared to the soil cover. The gradient observed on field indicate a really low diffusivity value for the soil cover. Since the least observed temperature is below the soil cover it was not possible to select a particular value for thermal diffusivity of the waste to match the observed profile using a simple 1D analytical model.

4.2 Impact of aeration on temperature

A final measurement was carried out on BB11n on the day aeration had begun. The test was run after almost a whole month of the baseline measurements. The resulting temperature profile was much different from the baseline measurement. This could be attributed to the aeration process causing a redistribution of heat within the landfill. It is to be noted that the presented data show the landfill temperatures after about 2 hours of aeration. During the initial 2 hours of aeration the temperature profile was changing quite frequently with time and reached an equilibrium temperature, as depicted in figure 4.13(Mean1 corresponds to before aeration and Mean 2 after aeration). The mean temperature within the well indicated in the graph suggest that the well temperatures reduced by 0.5 degrees upon the start of aeration. What is particularly seen is the the wells minimum and maximum values increase and reduced to form a more constant temperature profile within the well. Such behaviour of temperature profile where the temperature averages out can be explained by suggesting that the initial aeration has caused a re-circulation of the heat within the well by gas phase convection alone.

A conceptual model can be formulated based on heat equations on Chapter 2 to model the landfills temperature behaviour during the initial phases of aeration. If heat re-circulation is the cause of the temperature profile, heat entering and leaving the system would be controlled as function of rate of aeration. Thereby a second heat flux term in the heat equation is required to take into consideration would the convective transport of heat by air moving in and out of the system. While the first heat flux term is a function of diffusion of heat within the soil.

This process of aeration if applied to an anaerobic system could result in elevated temperature in the range above 50 deg C. Even though aeration has suggested elevated temperatures the landfills are also known to cool down subsequent to the decline of the rate of decomposition process, which is in the range of 20 to 40 deg C. Thereby resulting a net heating or cooling in the range of 3 deg C over the year [11]. This range from previous research provides some confidence in the ranges of temperature to be expected during the aeration phase.

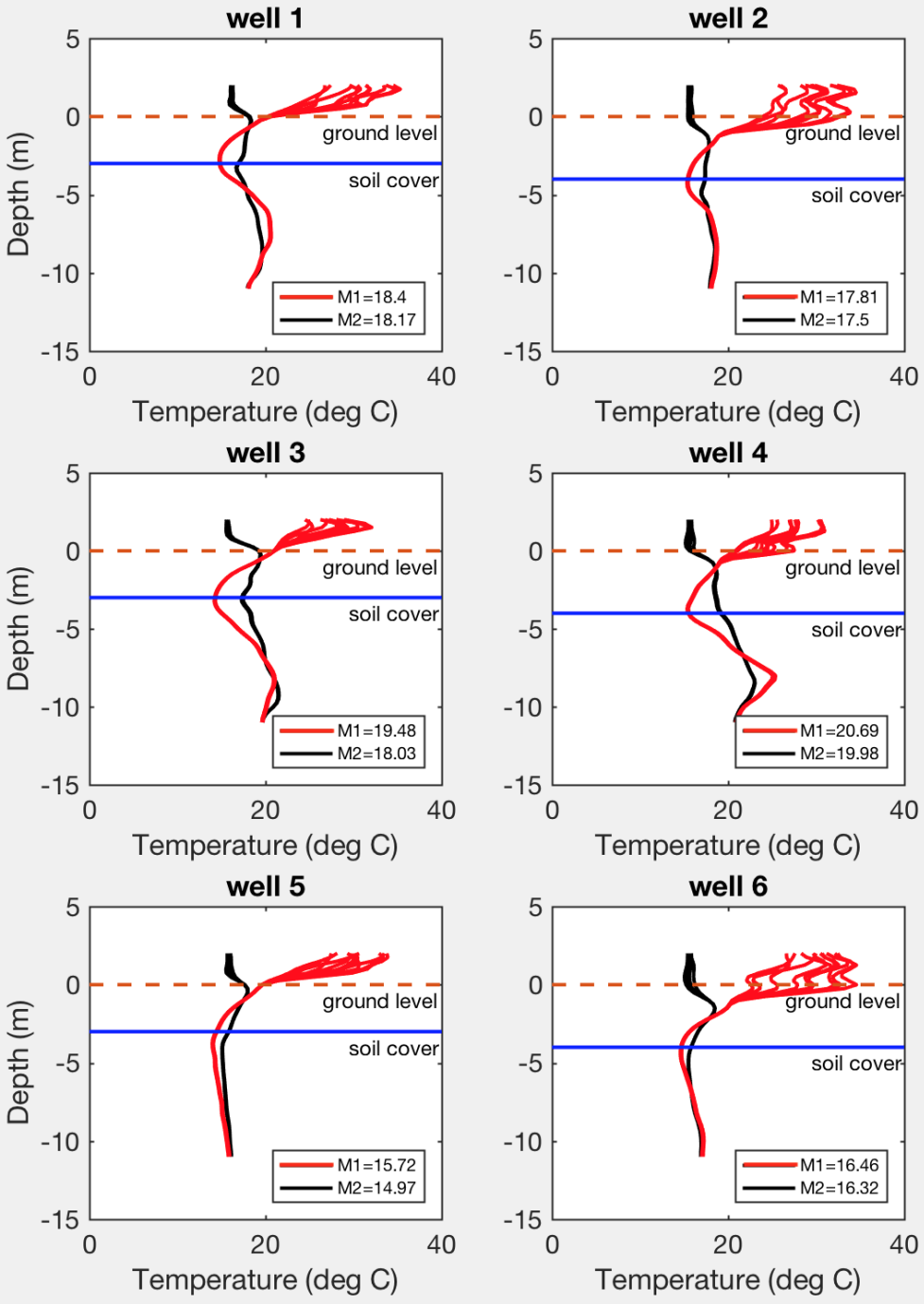

FIGURE 4.13: Temperature readings before and after aeration, M1 (deg C) corresponds to the mean well temperature before aeration and M2(deg C) the mean right after aeration began

Chapter 5

Conclusion

Distributed Temperature Sensing can enhance temperature sensing and monitoring for landfills. For this study, a distributed temperature sensing system has been applied to a full scale landfill at multiple locations. The distributed network provides a continuous monitoring system which is easy to use, while simultaneously providing high accuracy readings. The DTS instrument was capable of providing highly accurate temperature readings in the range of 0.02 deg C. Higher acquisition time results in an increase in accuracy and viable to use for long term measurements in the range of weeks to months. The shorter acquisition times are best used for real time monitoring and the accuracy achievable reduces to an order of 0.5 deg C.

The errors in temperature readings are a result of uncertainty in the position of fiber in space and the losses experienced by the cable during installation. Validation baths can be used to rectify installation losses while a depth matching algorithm can address the uncertainty of the fiber in space.

The landfill can be divided into three zones, the surface, soil cover and waste body. The surface temperature fluctuate heavily, with the temperatures within the wells staying relatively the same. A match is found between one-dimensional analytical heat formulation with two layers of soil and field data from the landfill. The analysis indicate that waste body was still generating heat and possibly could be a result of bio-activity. But detailed model is required to infer soil wastes thermal properties.

The initial phase of aeration caused the heat to re-distribute more homogeneously. This change was however not a result of heat generation but more likely associated to re-circulation of heat within the well by gas convection. The sudden change caused only a slight decrease in mean temperatures(reduced by 0.5 deg C). Major changes in heat due to enhanced activity as a result of aeration has not yet been captured at the fields.

This system can now be applied to quantify heat capacity of the landfill once the landfill begins to heat up as result of aerobic decomposition. Post aeration data along with

baseline measurements can provide insight into change of emission potential of landfill. Using glass fibers in landfills is quite clearly an upgrade from previous discreet temperature sensors used in the field, the used glass fibers are both robust and inexpensive to install. Even though installation of cables are relatively time-consuming, the trade-off, is the ease of carrying out tests for monitoring temperatures in harsh conditions.

Chapter 6

Recommendations

- Visual representation of spatially scattered data is another field of study which can be implemented into this project for future use. An important task in geoscience is the interpolation of scattered spatial data. By using methods of 3D kriging along with the high resolution DTS data it can be possible to generate a high resolution thermal picture of the landfill.[20]
- Many numerical models have been developed around a landfill, once the system is calibrated to achieve high accuracy it is advised to use methods of data assimilation to increase model performance.
- Through inverse modelling, complex models can be calibrated. However, significant uncertainties in certain parameters, initial conditions and modelled states remain due to lack of sufficient measurement data and fundamental information [4]. To improve the predictive power of these models, the uncertainty in these models should be minimized.An ideal solution is developing a modeling framework [3] for predicting emission potential in landfills in which model uncertainty is minimal given the available data and information. However, still significant uncertainty remains in the prediction of emission potential mainly because of uncertainty in parameters and initial conditions relating to water content and biological activity. Which can be significantly reduced by using temperatures from the DTS.Using techniques of inverse modelling with obtained data from the DTS one can improve the prediction/estimation of the emission potential.
- Literature in the field of landfills and temperature have been studied for many years now. It is important that the network installed be monitored on a continuous basis such that obtained readings are comparable to already existing models and theories. In order to do so, it is important to provide infrastructure to protect the instrument along with a higher standard calibration bath such that instrument drift can be accounted for during long test measurements. Calibration baths in this research were used only to test for instrument accuracy. Since accuracy was achieved in the forward and reverse cables in a

double ended configuration machine did not need to be further calibrated. But it would be in the best interest of future research to install a more robust calibration bath that maintains a constant temperature.

- Installing cables in aeration wells and connected them on surface has a lot of drawbacks namely bends at the bottom, splices at the entry, well retaining its profile etc. In order to avoid such issues it is advised that the cables be installed during waste placement for future requirements. Placing cables one the surface prior to placing waste would result in a network that would not have a high bending radius or number of splices.

- DTS system used for this research provides temperature reading based on Raman-backscatter. If the study needs to be extended to even detecting strain or settlement within the landfill it is advised to switch to a BOTDA/BOTDR method which analysis both strain and temperature.

Appendix A

An Appendix

A.1 Thermal Gradients - Visual Representation

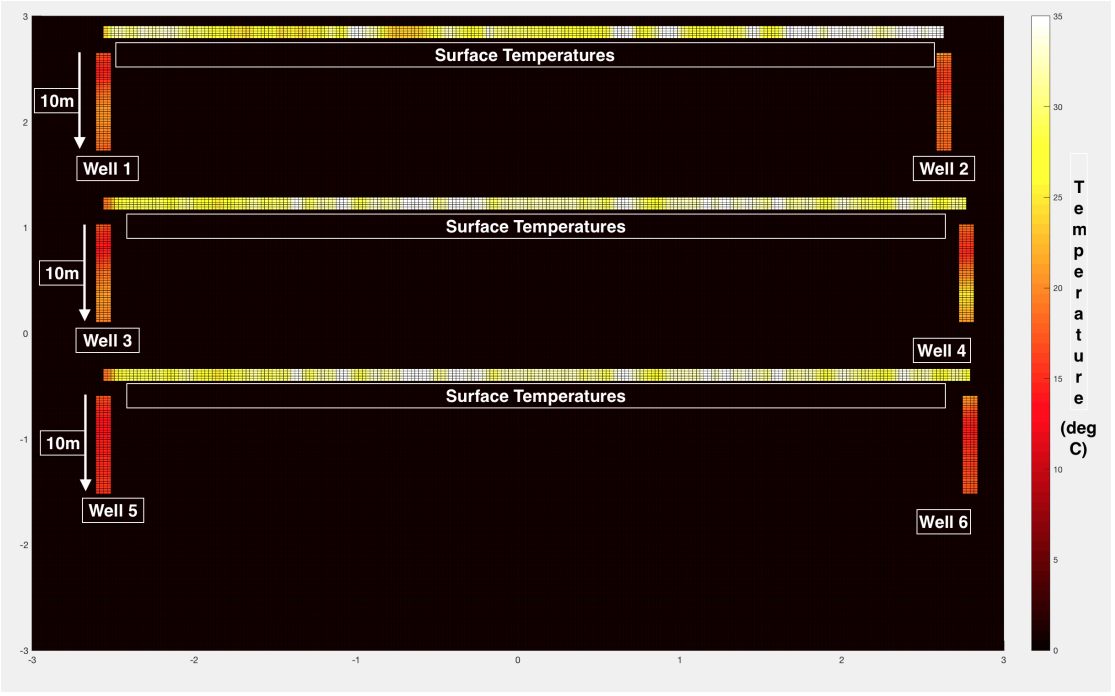

FIGURE A.1: BB11z temperature gradients

A.2 Equipment details

Equipment name : XTS

Manufacturer name: Silixa

Power requirements of DTS

Number of Channels: 4

Nominal Voltage Range +12 to +24VDC Power Rating Measuring 47W Power Rating Idle 15W Absolute Minimum Voltage +11VDC Absolute Maximum Voltage +36VDC

SLT STA with E-Glass

SLT STA with E-Glass 2 to 24 fibre OM1, OM2, OM3, OM4 multimode or OS1/OS2 (ITU-T G.652D) singlemode 250 µm single loose tube metallic armoured internal/external rodent resistant duct and direct burial cables with E-glass strength members, and Low Smoke Zero Halogen (LSZH) or High Density Polyethylene (HDPE)jacket.
The single loose tube cables consists of 2 to 24, 250 µm optical fibres in a single gel filled loose tube with longitudinally applied E-glass non metallic strength members, Corrugated Steel Tape (CST) armouring and LSZH or HDPE jacket.

Features

- Choice of fibre types
- Colour coded fibres
- CST armouring for enhanced impact, crush and rodent resistance
- Compact 250 µm loose tube construction
- Flame retardant LSZH jacket for enhanced fire performance or HDPE jacket for environmental protection and water permeation resistance

Applications

- Suitable for internal/external duct and direct burial applications
- Suitable for environments where impact protection is required
- Ideal for intra building links in campus environments

Specification

Parameter	Unit	Value
Crush	N/100mm	2000
Strength member		E-glass
Storage temperature	oC	-20 to 60
Installation temperature	oC	-20 to 60
Operating temperature	oC	-20 to 60
Nominal weight 2f to 12f	kg/km	LSZH 95 HDPE 73
Nominal weight 14f to 24f	kg/km	LSZH 110 HDPE 86
Fibre count	n	2, 4, 6, 8, 12, 16 & 24
Nominal outer diameter 2f to 12f	mm	8.5 ±0.3
Nominal outer diameter 14f to 24f	mm	9.2 ±0.3
Maximum tensile load (Short Term)	N	1000
Maximum tensile load (Long Term)	N	500
Minimum bend radius	mm	Installed 10D
Minimum bend radius	mm	Loaded 20D
Drum length	km	2 or 4
Plywood drum dimensions (Flange,Barrel,Width) 4km 2f to 12f	mm (approx)	F1000, B510, W690
Drum weight with cable 4km 2f to 12f	kg (approx)	LSZH 398 HDPE 310
Plywood drum dimensions (Flange,Barrel,Width) 4km 14f to 24f	mm (approx)	F1100, B500, W690
Drum weight with cable 4km 14f to 24f	kg (approx)	LSZH 461 HDPE 365

FIGURE A.2: Fiber optic cable Datasheet

TABLE A.1: BB11n field details

S.no	1			
Field location	Braambergen			
Field number	1			
Number of wells	6			
	Bottom	**Length of well1**	**Index**	**Mean Temperature (bottom 10m)**
Well 1/B4	59.255	11.948	438	19.13
Well 2/B3	136.786	10.677	738	17.5
Well 3/D4	300.236	11.948	1386	18.03
Well 4/D3	379.038	10.931	1691	19.98
Well 5/F4	541.726	11.693	2335	14.97
well 6/F3	621.036	10.422	2642	16.32

TABLE A.2: BB11z field details

S.no		2		
Field location		Braambergen		
Field number		2		
Number of wells		6		
	Bottom	**Length of well1**	**Index**	**Mean Temperature (bottom 10m)**
Well 1/Q7	48.3	12.5	191	13.61
Well 2/Q9	120	11	493	12.9
Well 3/O7	244.8	12.5	964	13.59
Well 4/O9	317	12.5	1248	13.41
Well 5/M7	438	12.5	1724	16.49
well 6/M9	509.6	12.5	2006	13.95

TABLE A.3: W field details

S.no		3		
Field location		Wieringermeer		
Field number		1		
Number of wells		6		
	Bottom	**Length of well1**	**Index**	**Mean Temperature (bottom 10m)**
Well 1/45	39.29	12.4	154	18.25
Well 2/43	105.13	12	414	15.93
Well 3/65	197.41	12.9	778	15.8
Well 4/63	264	12.9	1039	17.17
Well 5/85	356.284	13.1	1401	16.49
well 6/83	420.343	13.1	1655	15.82

Bibliography

[1] Royal Haskoning/IFAS. Feasibility study on sustainable emission reduction at the existing Kragge and Wieringermeer landfills in the Netherlands, generic report: Processes in the waste body and overview of enhancing technical measures". final report, March 2009.

[2] Boyd A. McKew, Alex J. Dumbrell, Joe D. Taylor, Terry J. McGenity, and Graham J.C. Underwood. Differences between aerobic and anaerobic degradation of microphytobenthic biofilm-derived organic matter within intertidal sediments. *FEMS Microbiology Ecology*, 84(3):495–509, 2013. ISSN 1574-6941. doi: 10.1111/1574-6941.12077. URL http://dx.doi.org/10.1111/1574-6941.12077.

[3] Andr G. van Turnhout, Christian Brandsttter, Robbert Kleerebezem, Johann Fellner, and Timo J. Heimovaara. Theoretical analysis of municipal solid waste treatment by leachate recirculation under anaerobic and aerobic conditions. *Waste Management*, 2017. ISSN 0956-053X. doi: https://doi.org/10.1016/j.wasman.2017.09.034. URL http://www.sciencedirect.com/science/article/pii/S0956053X1730702X.

[4] Karline Soetaert, Thomas Petzoldt, R Woodrow Setzer, et al. Solving differential equations in r: package desolve. *Journal of Statistical Software*, 33(9):1–25, 2010.

[5] O Braissant, G Bonkat, Dieter Wirz, and A Bachmann. Microbial growth and isothermal microcalorimetry: growth models and their application to microcalorimetric data. *Thermochimica acta*, 555:64–71, 2013.

[6] Abhisek Ukil, Hubert Braendle, and Peter Krippner. Distributed temperature sensing: review of technology and applications. *IEEE Sensors Journal*, 12(5):885–892, 2012.

[7] James J Smolen and Alex van der Spek. Distributed temperature sensing.

[8] R Clément, Marc Descloitres, T Günther, L Oxarango, C Morra, J-P Laurent, and J-P Gourc. Improvement of electrical resistivity tomography for leachate injection monitoring. *Waste Management*, 30(3):452–464, 2010.

[9] Nazli Yeşiller, James L Hanson, and Wei-Lien Liu. Heat generation in municipal solid waste landfills. *Journal of Geotechnical and Geoenvironmental Engineering*, 131(11):1330–1344, 2005.

[10] Charles JR Coccia, Ranjiv Gupta, Jeremy Morris, and John S McCartney. Municipal solid waste landfills as geothermal heat sources. *Renewable and sustainable energy reviews*, 19:463–474, 2013.

[11] N Yeşiller, James L Hanson, and H Yoshida. Landfill temperatures under variable decomposition conditions. In *Geo-Frontiers 2011: Advances in Geotechnical Engineering*, pages 1055–1065. 2011.

[12] SC Steele-Dunne, MM Rutten, DM Krzeminska, M Hausner, SW Tyler, J Selker, TA Bogaard, and NC Van de Giesen. Feasibility of soil moisture estimation using passive distributed temperature sensing. *Water Resources Research*, 46(3), 2010.

[13] A. Young, Great Britain. Department of the Environment. Wastes Technical Division, and D. Davies. *Applications of Computer Modelling to Landfill Processes*. The technical aspects of controlled waste management. Great Britain, Department of the Environment, Wastes Technical Division, 1992. URL https://books.google.nl/books?id=qlgXMwEACAAJ.

[14] James L Hanson, Nazlı Yeşiller, and Nicolas K Oettle. Spatial and temporal temperature distributions in municipal solid waste landfills. *Journal of Environmental Engineering*, 136(8):804–814, 2009.

[15] Lindsay Tallon and Mike OKane. Applying distributed temperature sensing to the heap leach industry.

[16] Scott W Tyler, John S Selker, Mark B Hausner, Christine E Hatch, Thomas Torgersen, Carl E Thodal, and S Geoffrey Schladow. Environmental temperature sensing using raman spectra dts fiber-optic methods. *Water Resources Research*, 45(4), 2009.

[17] Mark B Hausner, Francisco Suárez, Kenneth E Glander, Nick van de Giesen, John S Selker, and Scott W Tyler. Calibrating single-ended fiber-optic raman spectra distributed temperature sensing data. *Sensors*, 11(11):10859–10879, 2011.

[18] Nick Van De Giesen, Susan C Steele-Dunne, Jop Jansen, Olivier Hoes, Mark B Hausner, Scott Tyler, and John Selker. Double-ended calibration of fiber-optic raman spectra distributed temperature sensing data. *Sensors*, 12(5):5471–5485, 2012.

[19] F Suárez, JE Aravena, MB Hausner, AE Childress, and SW Tyler. Assessment of a vertical high-resolution distributed-temperature-sensing system in a shallow thermohaline environment. *Hydrology and Earth System Sciences*, 15(3):1081, 2011.

[20] Wolfram Rühaak. 3-d interpolation of subsurface temperature data with measurement error using kriging. *Environmental Earth Sciences*, 73(4):1893–1900, 2015.